



## QUIETMED – Joint programme on noise (D11) for the implementation of the Second Cycle of the MSFD in the Mediterranean Sea.

# quietMED

### Deliverable

D3.3 Best practice guidelines on acoustic modelling and mapping.

<b>Deliverable:</b>	D3.3 Best practice guidelines on acoustic modelling and mapping
<b>Document Number:</b>	QUIETMED - D3.3
<b>Delivery date:</b>	5 <sup>th</sup> December 2018
<b>Call:</b>	DG ENV/MSFD Second Cycle/2016
<b>Grant Agreement:</b>	No. 11.0661/2016/748066/SUB/ENV.C2

#### List of participants:

No	Participant organization name	Participant short name	Country
1	Centro Tecnológico Naval y del Mar	CTN	Spain
2	Instituto Español de Oceanografía	IEO	Spain
3	Universitat Politècnica de València	UPV	Spain
4	Service Hydrographique et Océanographique de la Marine	SHOM	France
5	Ispra Istituto Superiore per la Protezione e la Ricerca Ambientale	ISPRA	Italy
6	Inštitut za vode Republike Slovenije/Institute for water of the Republic of Slovenia	IZVRS	Slovenia
7	Permanent Secretariat of the Agreement on the Conservation of Cetaceans of the Black Sea, Mediterranean Sea and Contiguous Atlantic Area	ACCOBAMS	Monaco
8	The Conservation Biology Research Group, the University of Malta	UoM	Malta
9	Institute of Oceanography and Fisheries	IOF	Croatia
10	Foundation for Research and Technology – Hellas	FORTH	Greece

DISSEMINATION LEVEL	
PU: Public	x
PP: Restricted to other programme participants (including the Commission Services)	
RE: Restricted to a group specified by the consortium (including the Commission Services)	
CO: Confidential, only for members of the consortium (including the Commission Services)	

Company/Organization	Name and Surname
FORTH	Michael Taroudakis, Emmanuel Skarsoulis, Panagiotis Papadakis, George Piperakis
ACCOBAMS	Alessio Maglio and Achraf Drira (SINAY) Cédric Gervaise (CHORUS)
SHOM	Florent Le Courtois, Emeric Bidenbach

*©The QUIETMED Project owns the copyright of this which is supplied confidentially and must not be used for any purpose other than that for which it is supplied. It must not be reproduced either wholly or partially, copied or transmitted to any person without authorization. This document reflects only the authors' views. The author is not responsible for any use that may be made of the information contained herein.*

Table of Contents

**1 Introduction..... 7**

**2 Context and objectives..... 9**

**3 Noise mapping..... 10**

**4 Shipping noise modelling. .... 11**

**4.1 The shipping noise prediction components..... 11**

        4.1.1 Description of the underwater acoustic environment..... 11

        4.1.2 Prediction of the sound source characteristics ..... 13

        4.1.3 Sound propagation modelling..... 24

        4.1.4 Representation of the ambient noise levels ..... 25

**4.2 Existing models predicting shipping sound in the sea ..... 25**

**4.3 Calibration with in situ measurements ..... 26**

**5 Practical implementation: Mapping of the shipping noise around the Balearic Islands . 27**

**5.1 Scientific procedure ..... 27**

**5.2 Study area and period ..... 29**

**5.3 Layer 1: Shipping – Information form ..... 30**

        5.3.1 Information on ships from AIS data ..... 30

        5.3.2 Source models..... 30

        5.3.3 Other sources properties as input data for the model: ship size, speed and depth... 32

**5.4 Layer 2: Environment – Information form..... 32**

        5.4.1 Bathymetry..... 33

        5.4.2 Sound speed profile ..... 33

        5.4.3 Geoacoustic properties of the bottom..... 35

**5.5 Layer 3: Computation Scheme – Temporal approach with Refined Transmission Losses 37**

        5.5.1 Selecting the best acoustic model..... 37

        5.5.2 Model set up ..... 38

        5.5.3 Running the model over the study period ..... 39

**5.6 Layer 4: Calibration and validation ..... 39**

**5.7 Layer 5: Results, formatting and displaying ..... 40**

        5.7.1 Noise screenshots in the Balearics ..... 41

        5.7.2 D11C2 Indicators: average noise levels and other statistics ..... 43

        5.7.3 Comparison of different setups ..... 46

        5.7.4 Comparison with a different modelling approach: Noise maps in the Balearics using probabilistic modelling..... 47

**6 Conclusions, perspectives, recommendations ..... 49**

**7 Literature..... 50**

**8 ANNEX I ..... 54**

List of figures

Figure 1: Top: Typical picture of AIS ship locations – 1177 ships – received from Marine Traffic ship tracking service over a duration of 30 minutes. Bottom: Ship locations from AIS and dead reckoning – 1521 ships – for the same time interval. .... 14

Figure 2: Ship emission levels reported by [Veirs et al. 2012] based on the analysis of recordings from 1582 ships in Haro Strait. Shipping noise source spectrum, 1/12-, and 1/3-octave levels. Source level (SL) spectra of the entire ship population in 1 Hz (solid), 1/12-octave (dashed), and 1/3-octave bands (dotted). Black curves are medians without absorption; red curves are medians with absorption. .... 16

Figure 3: Ship emission levels reported by [McKenna et al. 2012] based on the analysis of recordings from 29 ships in Santa Barbara Channel. Ship source levels for (a) container ships and vehicle carriers, (b) bulk carriers and open hatch cargos, and (c) three types of tankers. Top two series of figures show one-octave and 1/3 octave bands, with mean and standard errors. Bottom series shows the 1 Hz band levels. .... 16

Figure 4: Ship emission levels reported by [Simard et al. 2016] based on the analysis of recordings from 255 ships in St. Lawrence Seaway - measurements with 3 hydrophones, close to the requirements of the ANSI/ASA S12.64-2009 standard. Box-whisker plots of the third-octave ship SSLs by ship category estimated using the mean of all hydrophones. The notches are the medians; the bars are the 1st and 99th percentiles, and x are outliers. .... 17

Figure 5: Geometry for surface image solution. .... 17

Figure 6: Distribution of acoustic intensity (Lloyd’s mirror pattern) of a source at 10 m depth and frequency of 300 Hz. The source location is close to the upper left corner of the plot. .... 18

Figure 7: Schematic geometry of various opportunistic measurements, and in the ANSI/ASA S12.64-2009 standard (in blue). .... 19

Figure 8: Lloyd’s mirror pattern of a source at 5 m depth for a frequency of 100 Hz (left) and 200 Hz (right), with superposed beam aspects of 1°, 10°, 15°, 30° and 45°. .... 19

Figure 9: Lloyd’s mirror pattern of a source at 10 m depth for a frequency of 100 Hz (left) and 200 Hz (right), with superposed beam aspects of 1°, 10°, 15°, 30° and 45°. .... 20

Figure 10: Top: Lloyd’s mirror pattern of a source at 9 m depth for a frequency of 100 Hz. Middle: Transmission loss vs. range at a depth of 60 m for a frequency of 100 Hz. Bottom: Error in source level estimation at 100 Hz using the spherical spreading law. .... 21

Figure 11: Error in source level estimation due to Lloyd’s mirror effect in ANSI/ASA S12.64-2009 standard for various source depth and various frequencies. .... 22

Figure 12: Noise distribution (dB re 1  $\mu$ Pa<sup>2</sup>/Hz) in the Eastern Mediterranean Sea in summer propagation condition at 100 m depth and frequency 100 Hz for source depth of 9 m (top) and 3m (bottom). .... 24

Figure 13: Sources – Receiver’s configuration for the simulation of shipping noise. .... 28

Figure 14: Location of Cabrera Pilot Project in the Mediterranean Sea. .... 29

Figure 15: List of noise source of navigating ships. .... 31

Figure 16: SL estimates according to different methods (models). .... 31

Figure 17: Bathymetric dataset used for the present work (source: EmodNet). .... 33

Figure 18: Sampling points for temperature and salinity. .... 34

Figure 19: Sound speed profile obtained from temperature and salinity data at 12 points of measurement. .... 34

Figure 20: Seafloor geological nature (source EmodNet). .... 35

Figure 21: Absorption depending on porosity (left) and on the grain size (right). .... 36

Figure 22: Variability in results estimated with varying parameters for the same noise screenshot. Left pictures focus on the effect of the source model. Right pictures on the effect of bathymetry. The first row shows the same twice, as to better describe the great variability, and hence the sensitivity of the choice for assessment purposes. .... 42

Figure 23: SPL statistics in the Balearics for the 1/3 octave band centred at 63 Hz: average (arithmetic mean), median (50% Exceedance level) and loudest noise (5% Exceedance levels) at two depth layers. .... 44

Figure 24: Noise statistics in the Balearics: average (arithmetic mean), median (50% Exceedance level) and loudest noise (5% Exceedance levels) at three depth layers. .... 45

Figure 25: Effect of source models on estimated noise levels. .... 46

Figure 26. Sound pressure levels (SPL) from shipping activities for the month of January 2017 (in dB re 1  $\mu$ Pa) for the one-third octave bands centred at 63 Hz (left) and 125 Hz (right). Top panel: 12m depth. Bottom panel: 100m depth. ....48

**List of tables**

Table 1. Minimum and maximum values for sound speed and density measured in sediments .....36  
 Table 2. Theoretical effectiveness of the different modelling methods according to different combinations of input parameters: bathymetry, frequency range of interest, influence of environmental factors. RI = range-independent; RD = range-dependent. ....38  
 Table 3. Summary of results for noise screenshots.....40  
 Table 4. Summary of results for indicator maps. ....40

**Bibliography**

Commission, E. (2008). DIRECTIVE 2008/56/EC OF THE EUROPEAN PARLIAMENT AND OF THE COUNCIL of 17 June 2008 establishing a framework for community action in the field of marine environmental policy (Marine Strategy Framework Directive).  
 Commission, E. (2016). DG ENV/MSFD Second Cycle/2016. Brussels.  
 Commission, E. (2016). Gran Agreement No. 11.0661/2016/748066/SUB/ENV.C2. Brussels.  
 Commission, E. (2017) Commission Decision (EU) 2017/848 of 17 May 2017

### List of Abbreviations

CTN	Centro Tecnológico Naval y del Mar
IEO	Instituto Español de Oceanografía
UPV	Universitat Politècnica de València
SHOM	Service Hydrographique et Océanographique de la Marine
ISPRA	Ispira Istituto Superiore per la Protezione e la Ricerca Ambientale
IZVRS	Inštitut za vode Republike Slovenije
ACCOBAMS	Permanent Secretariat of the Agreement on the Conservation of Cetaceans of the Black Sea, Mediterranean Sea and Contiguous Atlantic Area
UoM	The Conservation Biology Research Group, the University of Malta
IOF	Institute of Oceanography and Fisheries
FORTH	Foundation for Research and Technology – Hellas
MSFD	Marine Strategy Framework Directive

## 1 Introduction.

The QUIETMED Project is funded by DG Environment of the European Commission within the call “DG ENV/MSFD Second Cycle/2016”. This call funds the next phase of MSFD implementation, in particular to achieve regionally coherent, coordinated and consistent updates of the determinations of GES, initial assessments and sets of environmental targets by July 2018, in accordance with Article 17(2a and 2b), Article 5(2) and Article 3(5) of the Marine Strategy Framework Directive (2008/56/EC).

The QUIETMED project aims to enhance cooperation among Member States (MS) in the Mediterranean Sea to implement the Second Cycle of the Marine Directive and in particular to assist them in the preparation of their MSFD reports by 2018 through: i) promoting a common approach at Mediterranean level to update GES and Environmental targets related to Descriptor 11 in each MS marine strategies ii) development of methodological aspects for the implementation of ambient noise monitoring programs (indicator 11.2.1) iii) development of a joint monitoring programme of impulsive noise (Indicator 11.1.1) based on a common register, including gathering and processing of available data on underwater noise. The Project has the following specific objectives:

- ✓ Achieve a common understanding and GES assessment (MSFD, Article 9) methodology (both impulsive and continuous noise) in the Mediterranean Sea.
- ✓ Develop a set of recommendations to the MSFD competent authorities for review of the national assessment made in 2012 (MSFD, Article 8) and the environmental targets (MSFD, Article 10) of Descriptor 11- Underwater Noise in a consistent manner taking into account the Mediterranean Sea Region approach.
- ✓ Develop a common approach to the definition of threshold at MED level (in link with TG Noise future work and revised decision requirements) and impact indicators.
- ✓ Coordinate with the Regional Sea Convention (the Barcelona Convention) to ensure the consistency of the project with the implementation of the EcAp process.
- ✓ Promote and facilitate the coordination of underwater noise monitoring at the Mediterranean Sea level with third countries of the region (MSFD Article 6), in particular through building capacities of non-EU Countries and taking advantage of the ACCOBAMS-UNEP/MAP cooperation related to the implementation of the Ecosystem Approach Process (EcAp process) on underwater noise monitoring.
- ✓ Recommend methodology for assessments of noise indicators in the Mediterranean Sea basin taking into account the criteria and methodological standards defined for Descriptor 11 (Decision 2010/477/EU, its revision and Monitoring Guidelines of TG Noise).
- ✓ Establish guidelines on how to perform sensor calibration and mooring to avoid or reduce any possible mistakes for monitoring ambient noise (D 11.2.1). These common recommendations should allow traceability in case the sensor give unexpected results and help to obtain high quality and comparable data.
- ✓ Establish guidelines on the best signal processing algorithms for the preprocessing of the data and for obtaining the ambient noise indicators (D 11.2.1).
- ✓ Implement a Joint register of impulsive noise (D11.1.1) and hotspot map at Mediterranean Sea Region level by impulsive noise national data gathering and joint processing.

Enhance collaboration among a wide network of stakeholders through the dissemination of the project results, knowledge share and networking.

To achieve its objectives, the project is divided in 5 work packages which relationships are shown in Figure 1.

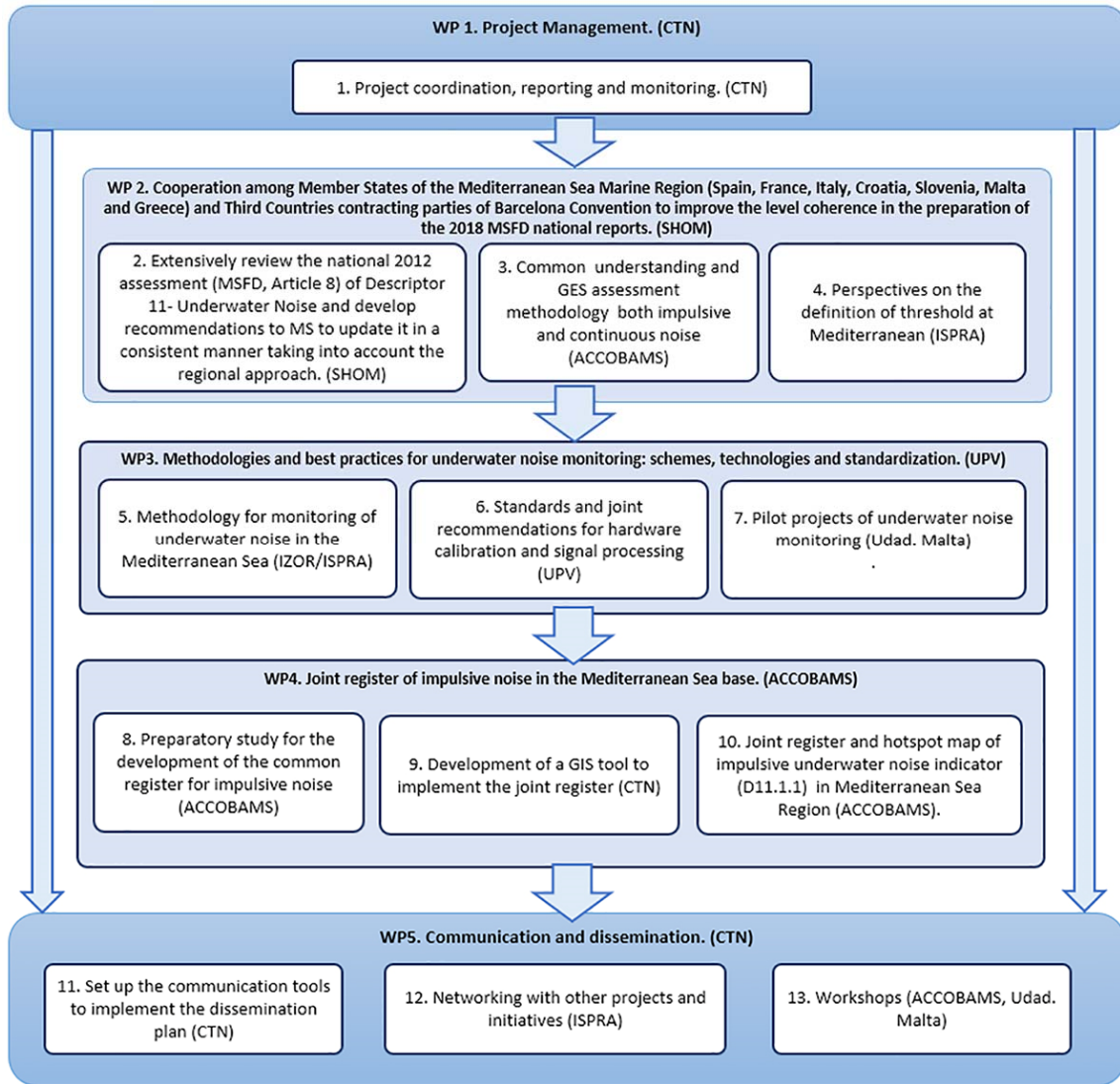


Figure 1. Work Plan Structure

The project is developed by a consortium made up of 10 entities coordinated by CTN and it has a duration of 24 months starting on January 2017.



## 2 Context and objectives.

Shipping noise is known to be the prevailing continuous noise in the marine environment at low and mid frequencies (Andrew et al., 2002; Dahl et al., 2007; Hildebrand, 2009; Wenz, 1962). Due to the propagation of sound at long ranges, individual ships may contribute to the ambient noise levels at these frequencies even if they navigate at long ranges from the measurement spot. Any attempt to reduce shipping noise in some area in order to achieve a better environmental status with respect to ambient noise, requires a thorough analysis of the existing situation, study of the prevailing sources of noise and their influence on the noise levels at the area of interest. As indicated by guidance from TG-Noise, a combination of in-situ measurements and noise mapping, including modelling would help in this respect (Dekeling et al. 2014).

The aim of this deliverable is to assess the state of the art in shipping noise modelling and mapping in the marine environment, as a preliminary study on the possibility of mapping underwater noise at low-to-mid frequencies in the Mediterranean.

It should be noted, that due to the complexity of the shipping noise modelling it is not possible at this stage to suggest specific procedures to overcome existing problems and build-up a robust and reliable shipping noise and subsequent noise-mapping model. Thus, in this report we will present the basic concepts of noise modelling and mapping, make reference to already reported solutions to shipping noise modelling, and address the main problems that the scientific community should solve in order to reach the final goal which is a reliable noise-mapping model.

Note that in accordance with the specifications set by the COMMISSION DECISION (EU) 2017/848 of 17 May 2017, for descriptor 11, related to monitoring anthropogenic continuous low-frequency sound in water, values to be concerned are *“Annual average, or other suitable metric agreed at regional or sub regional level, of the squared sound pressure in each of two ‘1/3-octave bands’, one centred at 63 Hz and the other at 125 Hz, expressed as a level in decibels in units of dB re 1  $\mu$ Pa, at a suitable spatial resolution in relation to the pressure. This may be measured directly, or inferred from a model used to interpolate between, or extrapolated from, measurements. Member States may also decide at regional or sub-regional level to monitor for additional frequency bands.”*

### 3 Noise mapping.

This term is referred to the representation of sound levels at a specific area using colour scales or contours. It has been used extensively for predicting noise levels in urban areas and has been a major subject of research and development in the framework of the EC Directive on noise control ([Directive 2002/49/EC](#)) .

Noise mapping can be based on measurements of the noise levels at various bands following a standard protocol in a specific area. However, noise mapping based on measurements only, can show a stationary condition of the noise. Noise mapping based on systematic measurements of noise at this area may predict variations of the noise levels at the different time zones or under different traffic conditions, but the efficient use of the maps is questionable, if the noise mapping is not assisted by modelling.

Thus, noise prediction models have also been used to assist the noise representation. In the air they are mainly based on ray theory and assume different traffic scenarios. The vehicles are represented as noise sources according to their type and size, and the sound propagation is calculated according to the actual geometry and the composition of the boundaries in the area.

This principle can also be applied in the marine environment to calculate noise maps in the areas of interest. Monitoring of the ambient noise in the sea is anyway one of the main objectives of MSFD (Descriptor 11) so noise mapping based on measurements and modelling is considered as an important task to be implemented and exploited by the national authorities.

Shipping noise modelling is an issue that has been considered over the last 30 years as a tool to predict the ambient noise level for the frequencies generated by ships. Efforts to estimate noise due to surface movement (wind generated noise) are also reported in literature. As the noise generated by the agitation of the sea-surface is mainly important at frequencies above 1000 Hz, which fall above the frequencies of priority for Descriptor 11, no mention will be made here on these types of models. Accordingly, this report will be focused on ship traffic noise modelling only.

## 4 Shipping noise modelling.

The mapping of marine traffic noise via simulation (modelling) is a complex task relying on many environmental inputs, descriptions of the spatio-temporal distribution of ships and their source levels, simplifying assumptions and model settings. An increasing number of ways to map shipping noise have been proposed by the scientific community (see section 3.2): on one hand, methods have been proposed that use approximated propagation laws that are fast and robust but lack environmental knowledge, on the other hand are refined simulation schemes, computationally expensive and sensitive to environmental inputs.

### 4.1 The shipping noise prediction components.

Shipping noise modelling in the sea involves several components:

- Description of the environment.
- Prediction of the ship movement in connection with the type and size of the ships.
- Prediction of the sound source characteristics.
- Sound propagation modelling.
- Representation of the ambient noise levels.

These components are briefly described below:

#### 4.1.1 Description of the underwater acoustic environment

The acoustic environment consists of the water layer and the sea-bed. For shallow water areas, knowledge of the sea-bed structure is important as sound propagation interacts with the sea-bed and the acoustic field is directly related to the sea-bed properties. The sea-bed can in principle be considered known as its changes are rather slow. Once a map of the sea-bed geometry and composition has been created, it can be used for most further modelling purposes. For deep water, the interaction of sound with the sea-bed is limited, so accurate knowledge of the sea-bed structure is not important for propagation purposes.

The water column is characterized by its temperature profile which can be translated into its sound speed profile. As the continuous monitoring of the physical profile of the water column is not practical, historical averages may be used when making predictions of seasonal variation in sound propagation in the marine environment.

Several databases are available for the description of the underwater acoustic environment of the Mediterranean Sea. Based on historical data and in order to simplify the calculations, for the FORTH model (see Annex 1) the seasonal variation of the temperature (and sound speed) profile is taken into account through a parametric model combining a linear velocity profile, 1510 m/s at the surface and 1570 m/s at 4000 m depth (typical winter profile in the Mediterranean), and a linear heating profile for the upper 150 m layer, starting from zero at

150 m depth and reaching its maximum at the surface. The velocity variation on the surface is taken between 1510 m/s (winter - zero heating) and 1545 m/s (summer - maximum heating).

In the past, there was no means to monitor ship movement in real time. Data bases of ship movement in specific areas were available indicating type of ships, course and speed. These data bases could be used to simulate a-posteriori ship distribution and movement in some area. The distribution of ships over a large area could be used to estimate the shipping noise at a specific location using appropriate propagation models.

Now it is possible to get through AIS, information on full real route followed by individual ships and the various traffic noise prediction models can use on-line data to determine the ship configuration at any time using appropriate procedures.

#### **4.1.1.1 Problems with the use of AIS data**

This section discusses problems with the use of AIS data. The Automatic Identification System (AIS) was introduced primarily as a collision avoidance aid. According to Regulation 19 of the International Maritime Organization's (IMO) International Convention for the Safety of Life at Sea (SOLAS) Chapter V (Carriage requirements for shipborne navigational systems and equipment), which became effective in January 2005, all ships with gross tonnage of 300 or more, and all passenger ships regardless of size, are required to carry VHF equipment broadcasting their static and dynamic data (static meaning ship name, type, navigation status etc., and dynamic meaning position fix, speed direction etc.), and receiving such data from nearby ships, within a few tens of km. The broadcast repetition period depends on navigation status, e.g. dynamic data are broadcasted every 2 to 10 seconds from ships underway, and every 3 minutes from ships at anchor, whereas static data are broadcasted every 6 minutes.

AIS signals are also received by land- and satellite-based receivers which in turn deliver AIS data to ship tracking services. Land based receivers have a reception range of a few tens of kilometres, depending on location and weather conditions. Satellite-based receivers offer larger spatial coverage but poor temporal coverage since they are on board polar satellites following low-altitude orbits with repetition periods of the order of 90 minutes. In this connection, data from satellite-based receivers that arrive within 2 hours are as “near-real-time”, between 2 and 12 hours as “typical”, and after 12 hours they are considered as delayed. While AIS data from land-based receivers are delivered in real time as they arrive, data from satellite-based receivers are delivered in batches, and they are usually resampled e.g. on a 1-minute basis.

The gaps in space and time of the AIS land- and satellite-based reception network, e.g. due to poor coverage of an area by land-based receivers or due to delayed receptions by satellite-based receivers, result in gaps in reported ship populations. A possible way to recover missing ships is by using a dead reckoning approach, using a data base containing all ships that have ever occurred in the area of interest with their last received static and dynamic characteristics and making projections based on these characteristics up to a time limit of 12 hours. Figure 1 demonstrates the significance of filling the gaps by presenting a typical population of ship locations based on AIS data (received from Marine Traffic in this case) over 30 minutes in the

Eastern Mediterranean (top panel) and the same data supplemented with additional ship locations from the dead-reckoning approach (bottom panel). On average, about 25% of the ships used in the near-real-time shipping noise prediction for the Eastern Mediterranean Sea developed at FORTH/IACM (<http://www.iacm.forth.gr/shipnoise>) see also Annex I, come from dead reckoning.

A further significant problem with noise modelling based on AIS data has to do with many small-size vessels which are abundant in certain sea areas, such as the Aegean or the Adriatic Sea, especially in summer, and which contribute significantly to the noise budget but do not carry AIS systems, such that they are not included in the scope of the ship tracking services. Even larger ships carrying AIS systems, but having them turned off, will not be included in the AIS data. All these vessels will not be accounted for in the modelling and this may in turn lead to underestimated predicted sound levels.

#### 4.1.2 Prediction of the sound source characteristics.

This is notoriously a difficult task. Although the type and speed of the ship can easily be obtained by information providers like AIS, their source levels cannot be considered with accuracy. Several publications address this problem and it is interesting to notice that in most cases they predict different sound source spectra even for the same type of ships, although they are based on measurements of the ship radiated noise.

There are several explanations about these differences, and the general message is that the modellers should be very careful in choosing the source spectrum of a ship of specific type and size, as the results of the noise modelling could be drastically different according to the type of sound source.

Recent studies on problems related to sound source characteristics appear in next sub-sections.

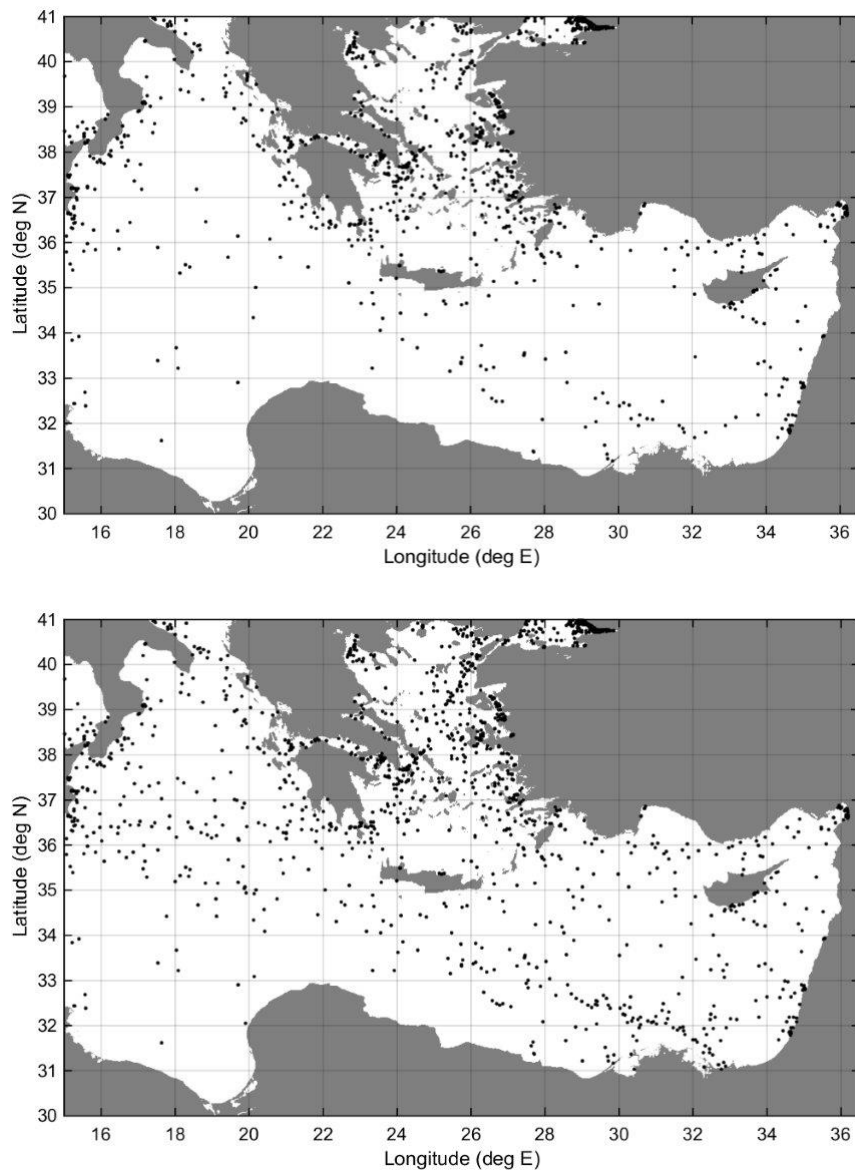


**Figure 2: Top: Typical picture of AIS ship locations – 1177 ships – received from Marine Traffic ship tracking service over a duration of 30 minutes. Bottom: Ship locations from AIS and dead reckoning – 1521 ships – for the same time interval.**

#### **4.1.2.1 Variability of source level data**

As already stated, the reliability of predicted noise levels due to shipping critically depends on the accuracy of the propagation model used, on the environmental representation (sound-speed distribution in the water column, bathymetry, geoacoustic characteristics) and last but not least on the source levels (acoustic signatures) of ships.

Ship source level is perhaps the only factor in the modelling process whose errors will be transferred directly to the prediction results, e.g. an increase by 10 dB in the source level will cause an overall increase by 10 dB in the acoustic field. Therefore, it is of critical importance to avoid systematic errors in the source levels.

It is well understood that different ships have different acoustic emission characteristics. Even one and the same ship may have different acoustic characteristics, depending on its load, its navigation status, its maintenance condition etc.

The measurement of acoustic signatures of ships can be carried out at acoustic ranges, nevertheless these facilities are commonly used for naval ships. The advent of the Automatic Identification System (AIS) has made opportunistic measurements of acoustic signatures possible. These measurements rely on fixed installations of one or more hydrophones in the vicinity of shipping lanes. When a ship passes its acoustic field is picked up and recorded and its location is obtained from the AIS. If the background noise in the area at the time of the measurement is low enough an estimate of the ship's acoustic signature is obtained taking into account the source-receiver distance and correcting for the corresponding transmission loss (propagation effect) – usually a variation of the spherical spreading law is used for the latter.

In the last decade there is a substantial body of literature reporting typical noise levels of various ship types. A basic problem has to do with the large variability of the reported source levels. An example of this variability is shown in Figs. 2-4. In Figure 2 the reported average source levels by [Veirs et al. 2012] are shown, based on the analysis of recordings from 1582 ships in Haro Strait. Taking for comparison the 1/3 octave band levels we see that the 1/3 octave band level at 100 Hz nears 160 dB re 1  $\mu\text{Pa}^2/\text{Hz}$  @ 1m.

In another study from the same period [McKenna et al. 2012] based on the analysis of recordings from 29 ships in Santa Barbara Channel, Figure 3, the average 1/3 octave band level at 100 Hz for various ship types are close to 170 dB re 1  $\mu\text{Pa}^2/\text{Hz}$  @ 1m, i.e. 10 dB higher than reported by [Veirs et al. 2012]. Both studies used single hydrophone installations. A more recent study by [Simard et al. 2016] based on the analysis of recordings from 255 ships in St. Lawrence Seaway, which tried to follow (albeit with deviations) the ANSI/ASA S12.64-2009 standard for the measurement of acoustic signatures, resulted in even higher source levels: the average 1/3 octave band levels at 100 Hz, Figure 4, are higher than 180 dB re 1  $\mu\text{Pa}^2/\text{Hz}$  @ 1m. These discrepancies of more than 20 dB is very large and as already mentioned translates directly into variations of the same amount in the predicted noise levels.



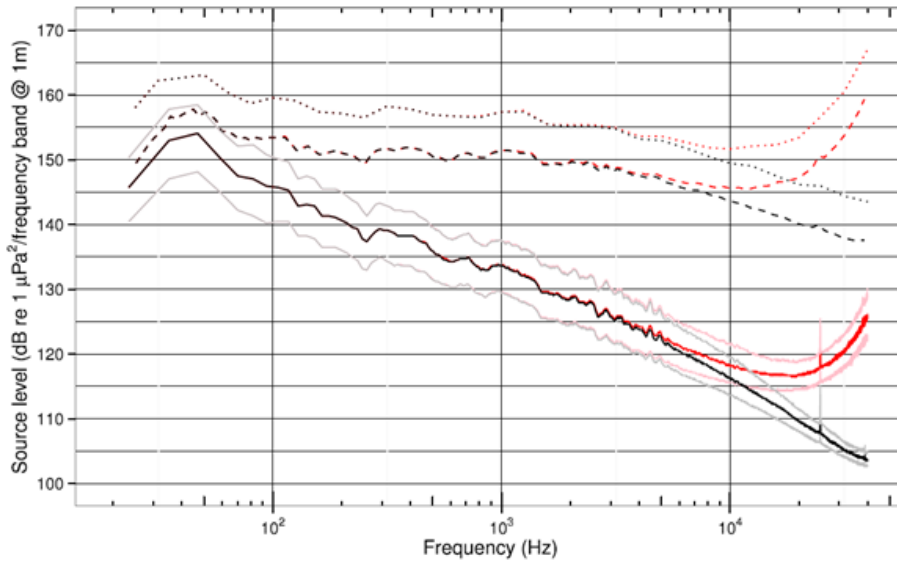


Figure 3: Ship emission levels reported by [Veirs et al. 2012] based on the analysis of recordings from 1582 ships in Haro Strait. Shipping noise source spectrum, 1/12-, and 1/3-octave levels. Source level (SL) spectra of the entire ship population in 1 Hz (solid), 1/12-octave (dashed), and 1/3-octave bands (dotted). Black curves are medians without absorption; red curves are medians with absorption.

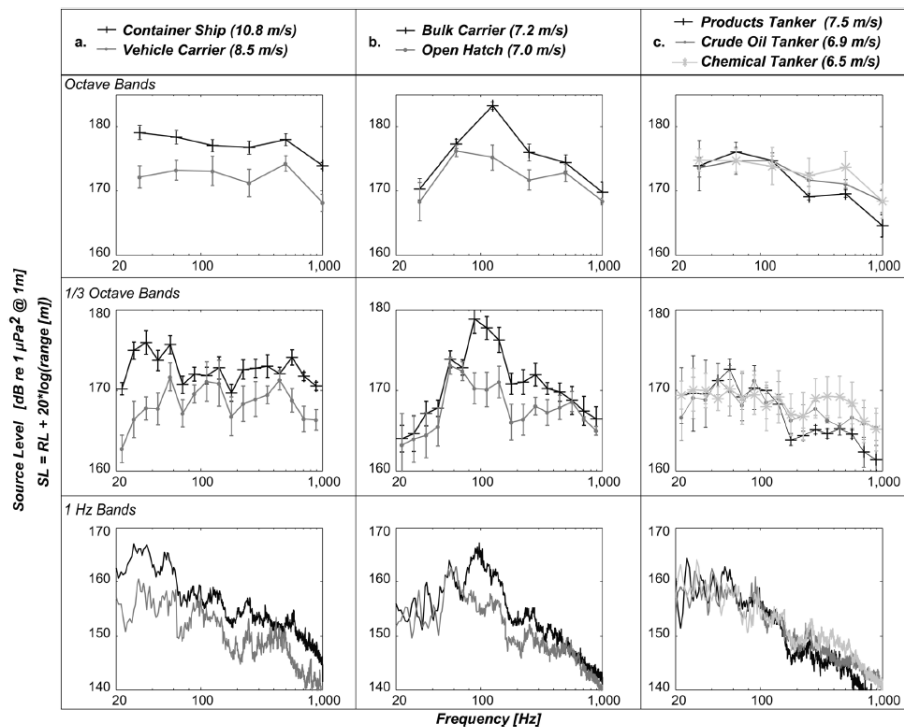


Figure 4: Ship emission levels reported by [McKenna et al. 2012] based on the analysis of recordings from 29 ships in Santa Barbara Channel. Ship source levels for (a) container ships and vehicle carriers, (b) bulk carriers and open hatch cargos, and (c) three types of tankers. Top two series of figures show one-octave and 1/3 octave bands, with mean and standard errors. Bottom series shows the 1 Hz band levels.



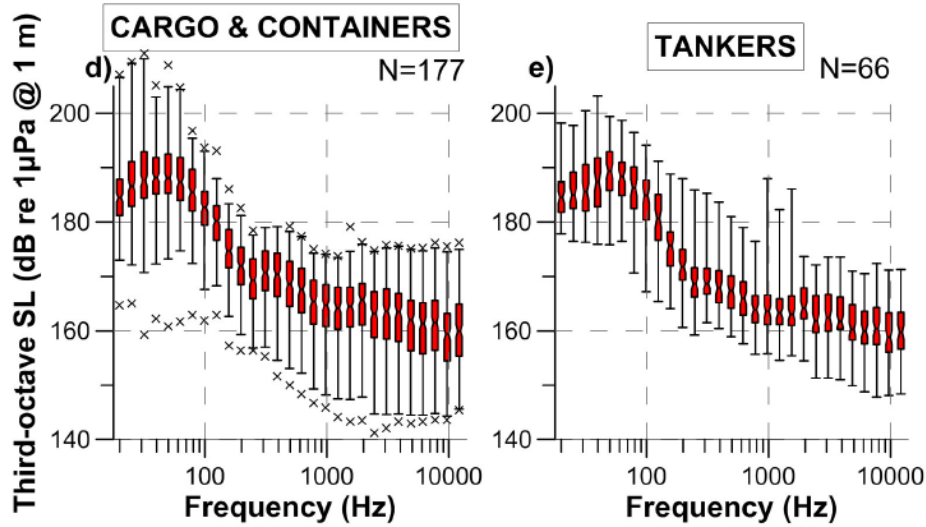


Figure 5: Ship emission levels reported by [Simard et al. 2016] based on the analysis of recordings from 255 ships in St. Lawrence Seaway - measurements with 3 hydrophones, close to the requirements of the ANSI/ASA S12.64-2009 standard. Box-whisker plots of the third-octave ship SSLs by ship category estimated using the mean of all hydrophones. The notches are the medians; the bars are the 1st and 99th percentiles, and x are outliers.

In a recent paper by [Gassmann et al. 2017] the divergence in the reported source levels in opportunistic measurements is assigned to the Lloyd’s mirror effect. The Lloyd’s mirror describes the acoustic field of a point source in the vicinity of a pressure-release surface such as the sea surface. The resulting acoustic field is the superposition of the acoustic field of a point source in free space and the acoustic field of its mirror image, subject to the condition for the vanishing of the total field at the pressure release surface, Figure 5 and Eq. (1).

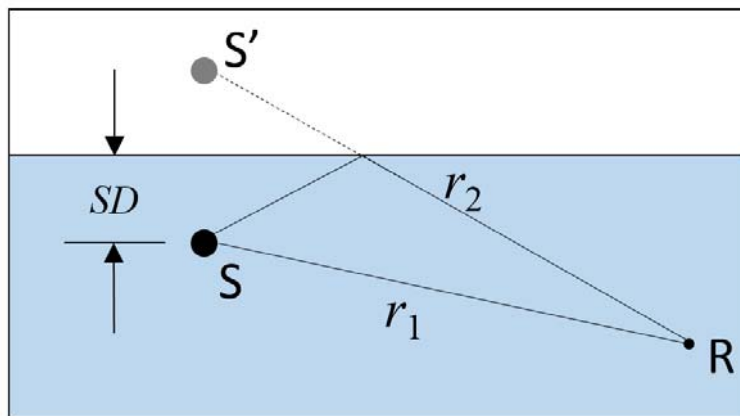


Figure 6: Geometry for surface image solution

The

$$P(r, z) = \frac{e^{ikr_1}}{r_1} - \frac{e^{ikr_2}}{r_2} \quad \text{where} \quad k = \frac{\omega}{c_0} = \frac{2\pi f}{c_0}$$

The resulting acoustic field depends on the source depth (SD) and the source frequency (f). A typical result is shown in Figure 6 for source depth of 10 m and frequency 300 Hz. It is seen that the acoustic field consists of a number of beams/lobes of high intensity (constructive interference of the two underlying fields) emanating from the source at specific elevation

angles, separated by shadow areas, i.e. areas of very low intensity (destructive interference), where the intensity drops with increasing distance from the source much faster than in simple spherical spreading. This means that in a measurement of the source level with a hydrophone located in a shadow area the source level will be considerably underestimated even if the correction with the spherical spreading law is made. The first shadow area is always close to the sea surface, in conformity with the pressure release condition. In this connection the beam aspect at which the measurement is made is of critical importance.

Taking into account that the Lloyd's mirror pattern changes with frequency and source depth (a decrease in frequency and source depth changes the number and geometry of the intensity beams) further complicates the situation when a single hydrophone is used; it is impossible to cover a wide frequency range sufficiently with a single hydrophone located at a particular depth and range. In this connection the ANSI/ASA S12.64-2009 standard for the measurement of acoustic signatures requires the use of three hydrophones located at beam aspects of 15°, 30° and 45° and averaging of the estimated levels, in order to overcome (at least partially) the Lloyd's mirror effect.

Figure 7 shows the geometry of various opportunistic measurement setups used in combination with the AIS to obtain source level estimates for commercial ships. It is seen that the vertical elevation of the hydrophone used by [Veirs et al. 2012] is about 0.2°, which is exceptionally small. In the setup used by [McKenna et al. 2012] the elevation angle is larger, about 10°. Finally in the setup by [Simard et al. 2017] the three hydrophones had beam aspects of 7°, 18° and 30°, close but not fully complying with the requirements of the ANSI/ASA S12.64-2009 standard. This gradual increase in the elevation angles of the above studies is the main reason for the gradual increase in the estimated source levels, taking into account that all studies used some variation of the spherical spreading law to account for the transmission loss.

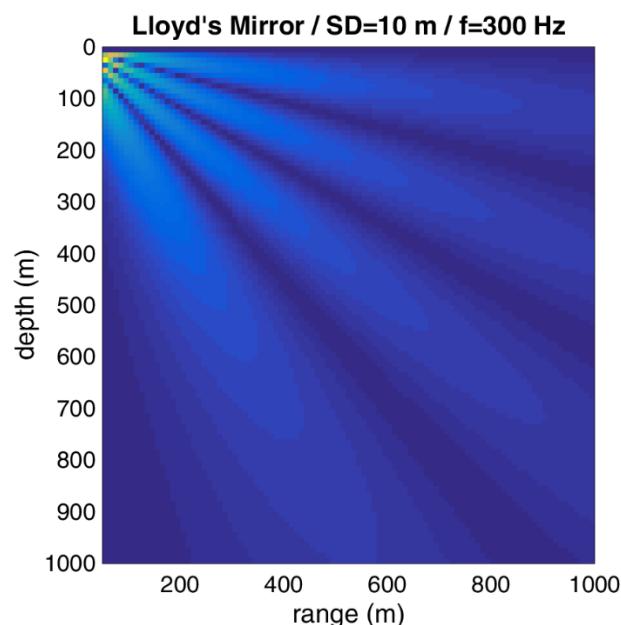


**Figure 7: Distribution of acoustic intensity (Lloyd's mirror pattern) of a source at 10 m depth and frequency of 300 Hz. The source location is close to the upper left corner of the plot.**

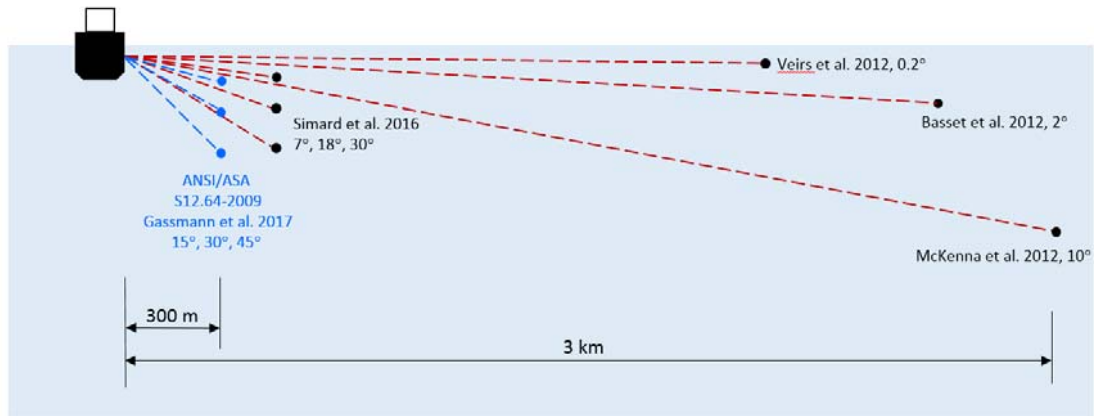


Figure 8: Schematic geometry of various opportunistic measurements, and in the ANSI/ASA S12.64-2009 standard (in blue).

Figure 8 shows the Lloyd’s mirror pattern of a source at 5 m depth for a frequency of 100 Hz and 200 Hz, with superposed beam aspects of 1°, 10°, 15°, 30° and 45°, the latter three corresponding to the ANSI/ASA S12.64-2009 standard. There is one intensity lobe at 100 Hz and 2 lobes at 200 Hz. In both cases the 1° beam aspect falls entirely in the shadow area close to the surface. This explains the lower source level values reported by [Veirs et al. 2012]. The 10° beam aspect [McKenna et al. 2012] is closer to the centre of the first lobe. This explains the larger source level values reported by these authors. Finally, the 15°, 30° and 45° beam aspects are even closer to or even intersect with the central sector of the first lobe. Of course, it is not possible for all the beam aspects to intersect with the intensity lobes, nevertheless the averaging of the three estimated source levels in dB results in a fair approximation of the true source level.

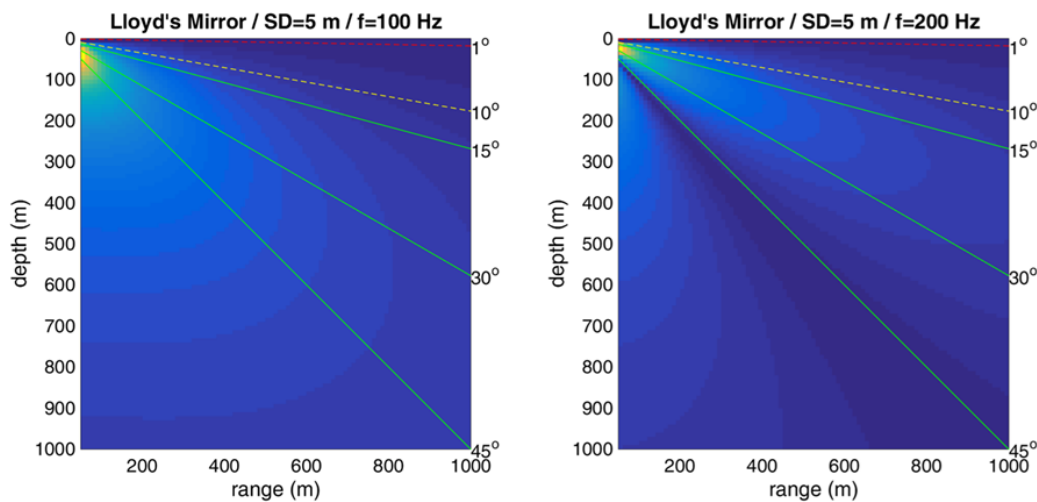


Figure 9: Lloyd’s mirror pattern of a source at 5 m depth for a frequency of 100 Hz (left) and 200 Hz (right), with superposed beam aspects of 1°, 10°, 15°, 30° and 45°.

Figure 9 is similar to Figure 8, the only difference being that the source is now at a depth of 10 m. This has led to an increase in the number of intensity beams, compared to the shallower source. The same comments apply as to the previous figure. With these two figures it becomes

evident that it is impossible to cover a wide frequency range sufficiently with a single hydrophone located at a particular depth and range. This is true even for the three hydrophones of the ANSI/ASA S12.64-2009 standard.

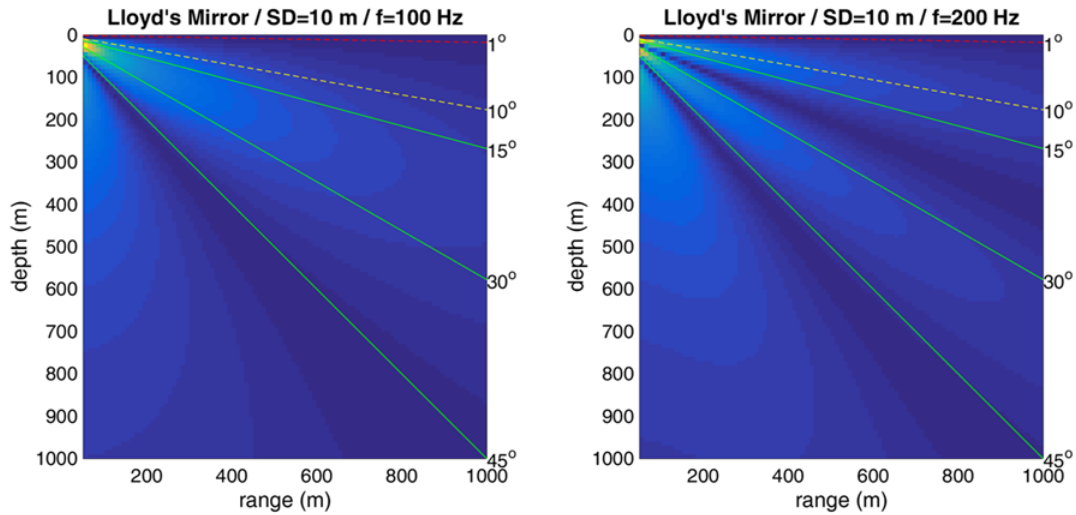


Figure 10: Lloyd's mirror pattern of a source at 10 m depth for a frequency of 100 Hz (left) and 200 Hz (right), with superposed beam aspects of 1°, 10°, 15°, 30° and 45°.

The top panel of Figure 10 shows the Lloyd's mirror pattern for source depth of 9 m and frequency 100 Hz, whereas the middle panel shows the transmission loss as a function of range  $r$  for a receiver (hydrophone) at 60 m depth (green line) compared to the spherical spreading law ( $20\log r$ , with  $r$  in meters). It is seen that the actual transmission loss (subject to the Lloyd's mirror effect) is much larger than the transmission loss in spherical spreading and increasing with range for ranges larger than 500 m. The bottom panel in Figure 10 shows the error in the source level estimation as a function of hydrophone range (assuming hydrophone depth 60 m) if the spherical spreading law is used to correct the measurements. E.g. for measurement at 1500 m from the source the error is -10 dB, i.e. the estimated source level is 10 dB lower.

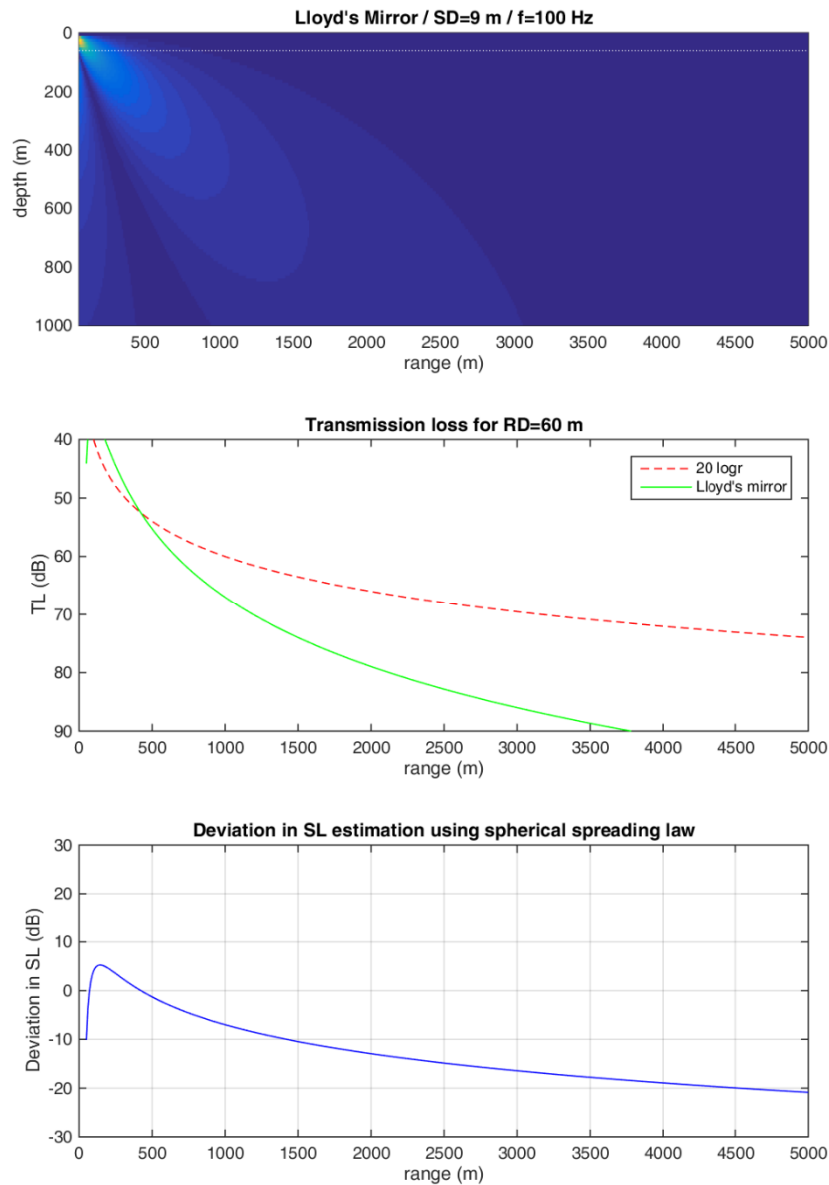


Figure 11: Top: Lloyd’s mirror pattern of a source at 9 m depth for a frequency of 100 Hz. Middle: Transmission loss vs. range at a depth of 60 m for a frequency of 100 Hz. Bottom: Error in source level estimation at 100 Hz using the spherical spreading law.

As already mentioned the Lloyd’s mirror effect has a strong impact on single hydrophone measurements, but it also affects multi-hydrophone measurements, even if they follow the ANSI/ASA S12.64-2009 standard, since the Lloyd’s mirror pattern changes with frequency and for some frequencies will be located in the shadow areas. Figure 11 quantifies the effect of the Lloyd’s mirror on the estimated source level with a hydrophone configuration complying with the ANSI/ASA S12.64-2009 standard for various source depths and various frequencies. The 3 hydrophones are assumed to be at a horizontal distance of 300 m from the source. It is seen that for the three frequencies considered (50, 100, and 200 Hz) and for source depths 3 m and above, there are positive deviations reaching about 5 dB and averaging around 2-3 dB.

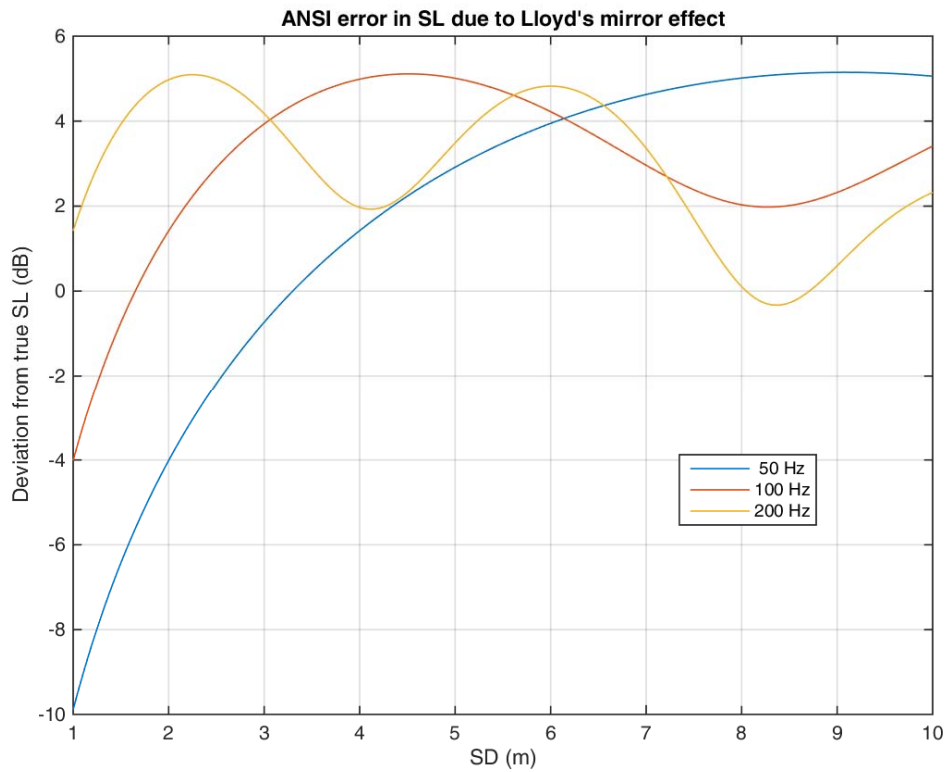


Figure 12: Error in source level estimation due to Lloyd’s mirror effect in ANSI/ASA S12.64-2009 standard for various source depth and various frequencies.

#### 4.1.2.2 Source depth

The primary mechanisms of emitted sound by a travelling ship are propeller cavitation and hull vibration due to operating ship engine and auxiliary machinery. Propeller cavitation takes place due to bubble formation and decay on the suction side of the propeller blades and it usually occurs when the blades are close to the surface (where hydrostatic pressure is low and favours cavitation). Therefore, the typical source depths for cavitation noise are relatively shallow (typically 2-3 m for larger vessels) corresponding to the depth of the propeller blades when they are closest to the surface. This depth can be approximated by the difference between the ship draught and the propeller diameter. On the other hand, the characteristic source depths for vibration generated noise are deeper and of the order of the ship draught averaging to 8-10 m for larger vessels.

Figure 12 shows the predicted noise levels at a frequency of 100 Hz and at a depth of 100 m in the Eastern Mediterranean Sea for summer propagation conditions generated by the same ship population used in [Skarsoulis et al. 2017], assuming two different values for the source depths: 9 m (top panel) and 3 m (bottom panel) – the source levels were exactly the same in both cases.

It is seen from this figure that there is a drop in the predicted noise levels in the case of the shallower sources, close to 10 dB. In other words, uncertainty about the source depth may cause significant uncertainty in the predicted noise levels of the order 10 dB. From the wave-theoretic normal-mode perspective this can be explained by the fact that the field excitation decreases as the source comes closer to a pressure release surface (the sea surface) where the propagation modes vanish. On the other hand, this behaviour points to the importance of using meaningful source depths for the various sources.

Even for one and the same ship the source depth may vary depending on the prevailing noise generating mechanism, e.g. a deeper source at lower speeds when vibrations are the main sources of noise and a shallower source at higher speeds when cavitation noise prevails.

A comprehensive model requires a more detailed description of the ship characteristics, including propeller features and relative importance of the various noise generating mechanisms at the various navigation conditions, that are today unavailable for virtually all of the world's ships. The IMO (International Maritime Organization) [IMO 2013] recently adopted guidelines to reduce noise from commercial ships, which recommends more detailed measurement of the acoustic emission characteristics of ships. More detailed ship characteristics may become available in future.



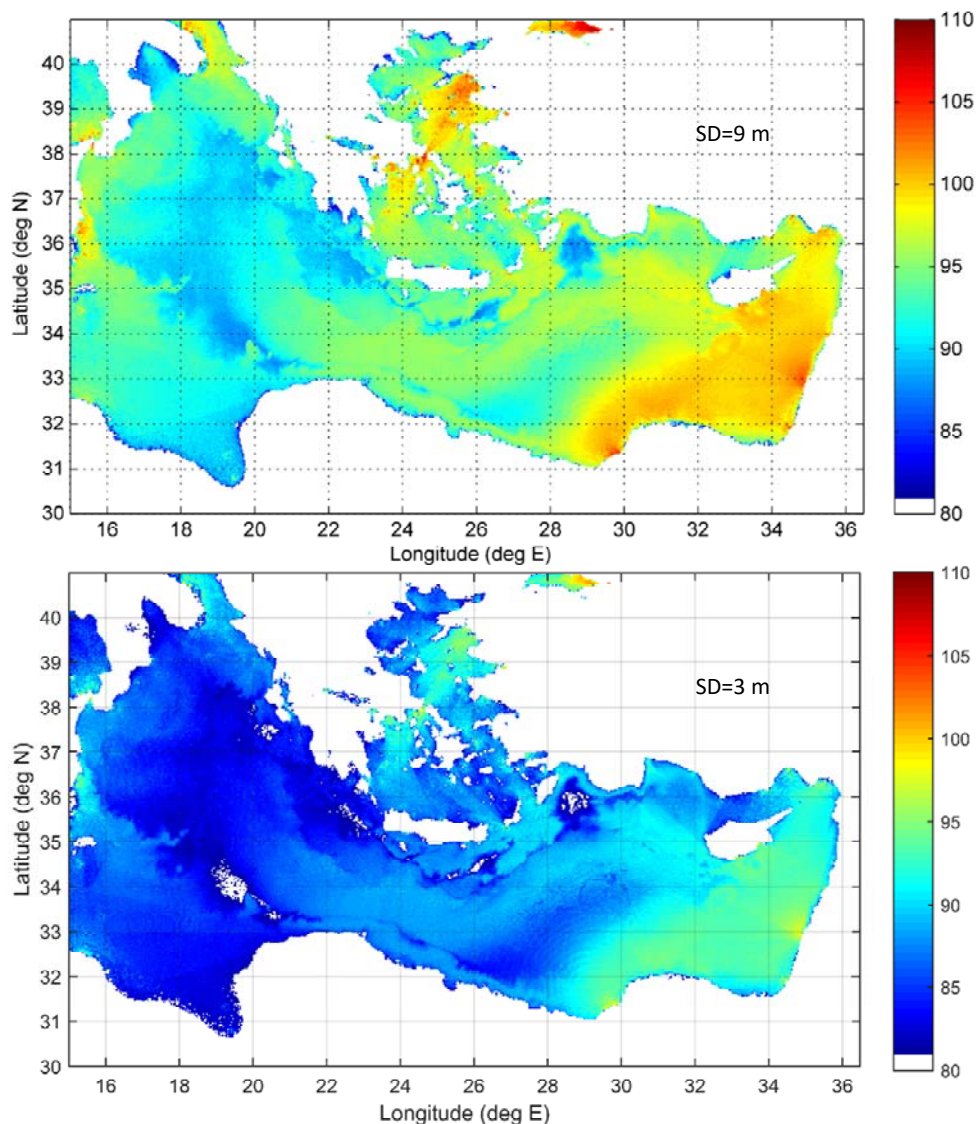


Figure 13: Noise distribution (dB re 1  $\mu\text{Pa}^2/\text{Hz}$ ) in the Eastern Mediterranean Sea in summer propagation condition at 100 m depth and frequency 100 Hz for source depth of 9 m (top) and 3 m (bottom).

### 4.1.3 Sound propagation modelling

Propagation modelling is also required if sound maps are to be generated. Reliable propagation models for underwater acoustics nowadays are mainly referred to either normal-mode propagation, parabolic approximations or to ray acoustics. These types of models can cover a great range of geometries and frequency ranges so they are considered appropriate for the task of ship traffic noise modelling. There is no need to go into details of these models that can be found in standard texts of underwater acoustics. In the annex of this deliverable the suggested models utilized in specific existing shipping noise modelling schemes will be mentioned.



It is not easy to perform propagation modelling due to the complexity of the geometry of the marine environment unless several assumptions are adopted for the simplification of the environment with minimum loss of prediction accuracy. For the frequencies of interest for shipping noise modelling, a normal-mode model seems to be appropriate in terms of accuracy. The environment is of course 3-D. However, a fully 3-D normal mode problem is not practical due to the complexity of the calculations. PE models could be used instead or, adiabatic normal modes calculations as in the case of the FORTH model can be a good compromise in this respect.

Considerable work is still needed before a specific propagation model for MSFD purposes can be recommended.

#### 4.1.4 Representation of the ambient noise levels

Mapping of ambient noise can use colours indicating noise levels. It is customary that high noise levels are represented by red colours, whereas low noise levels are represented by blue colours (see e.g. Figure 12). The representation of the noise levels is based in the calculation of the transmission loss from the source at a specific location and depth to the location of the measurement site.

## 4.2 Existing models predicting shipping sound in the sea

Several models are reported in literature or can be found on internet dedicated to the prediction of the shipping noise. A list of models or authors that have reported shipping noise models known to the authors of this report appear in the following table. Related references are mentioned in the Literature section of this report.

- ✓ *Taroudakis and Nicolaides, 1989*
- ✓ *Siderius and Porter, 2006*
- ✓ *ESME (Effect of Sound on the Marine Environment) & Animat, (Gisiner et al, 2006)*
- ✓ *Erbe et al, 2012, 2014*
- ✓ *SINAY - (Maglio et al., 2017, 2015)*
- ✓ *Porter et Henderson, 2013*
- ✓ *Folégot et al, 2012;*
- ✓ *Colin et al, 2015*
- ✓ *FORTH Model, 2016, 2017*
- ✓ *PSSEL (Probabilistic Shipping SEL modelling), Gervaise et al, 2015, Aulanier et al, 2017*
- ✓ *SHOM – Cabat, Le Courtois et al, 2016*
- ✓ *Redfern et al, 2017,*
- ✓ *Halliday et al, 2017*
- ✓ *Synthesis project UE BIAS*

The model developed at FORTH is briefly described in Annex 1.

### 4.3 Calibration with in situ measurements

As already explained, a variety of factors may affect the precision and the accuracy of models of shipping noise, including the natural variability or inaccuracy of inputs (e.g., the source level of ships, the sound speed profile), the lack of knowledge on certain input parameters (e.g., bottom characteristics and its geo-acoustics features), and the sensitivity of the models to the settings adopted. The systematic inclusion of in situ measurements will definitely help in the validation of the shipping sound propagation models, provided that most of the input parameters of the models are well calibrated.

Noise-modelling and mapping is not yet considered at a fully mature stage for the adoption of rigorous procedures to test the consistency of measurements and model results. However, thanks to the MSFD requirements, several programmes of in-situ measurements of shipping noise have started or will start in the near future in the EU and Mediterranean waters, and among them, the three pilot projects of QUIETMED. These measurements will sample the local sound levels around the measurement points, at the exception of mobile measurements made with drifting devices or gliders. The capability to extrapolate measured noise levels to larger and different areas is questionable. However, it is expected that they can help in testing a model procedure for the accreditation of the traffic noise models.

In the following chapter (Chapter 4), the report focuses on the pilot project of Cabrera, where a benchmarking of different solutions for shipping noise mapping has been carried out. The different approaches are presented, and the settings of the computational schemes are described. Finally, noise maps are shown, and variability factors are discussed.

## 5 Practical implementation: Mapping of the shipping noise around the Balearic Islands

In this chapter, we carry out a modelling exercise in the area of the pilot project of the island of Cabrera (Balearic Islands) foreseen in the framework of QUIETMED. This modelling exercise aims principally at producing noise maps in this pilot area by applying the recommendations contained in the TG-noise guidance; moreover, this work provides result that can be used as first baselines, and includes a benchmark of different processes for continuous noise mapping. This modelling is focussed on continuous anthropogenic noise generated by shipping, which is identified as the major contributor of anthropogenic noise into the marine environment.

The main modelling exercise was carried out by the team of the Underwater Acoustics Unit of SINAY, using the Big Data and HPC platform developed by the company<sup>1</sup>. The SHOM also contributed to the benchmark with noise maps produced using their model CABAT mentioned in the previous section.

### 5.1 Scientific procedure

The large scope of solutions for shipping noise modelling and mapping fall within 2 classes of methods:

- ✓ The temporal approach, for which a time step is chosen, and the trajectory of each ship is drawn. At each time step, each ship is located at its true location. The Transmission Loss (TL) is then computed from each ship to the range of receivers (a gridded 3D space with a vertical and horizontal resolution). The shipping noise at the receiver place, for each time step, is the sum of the contributions from each ship. Therefore, a time series of noise levels at the receiver place is built. This time series is then used to assess the cumulative or probability density function of the noise levels and their statistic moments (mean, standard deviation...);
- ✓ The probabilistic approach, for which a spatial grid is chosen and the shipping distribution is computed over this grid (ex : Number of hours per day of the presence of one ship in one pixel). Then this gridded distribution and the TL between each pixel centre and the receiver are used to compute directly the cumulative or probability density function of the noise levels and its statistics moments (mean, standard deviation...) without producing a time series.

---

<sup>1</sup> [www.sinay.fr](http://www.sinay.fr)

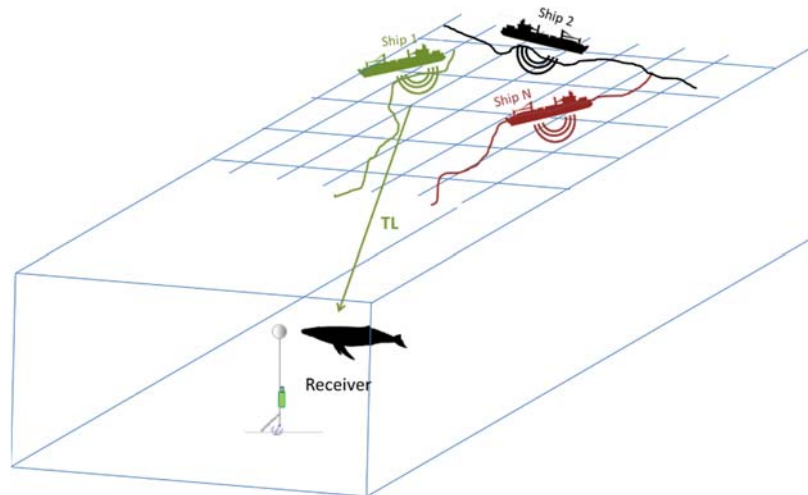


Figure 14: Sources – Receiver's configuration for the simulation of shipping noise

To carry out the propagation modelling a common information ground is necessary for either method. The common ground includes 5 categories of information (here referred to as layers, as presented at the beginning of chapter 3):

1. Layer 1 - Information on shipping: spatial and temporal distribution of shipping, source depth, levels, and emission frequency spectrum
2. Layer 2 - Propagation environment: bathymetry, sound speed profile, geoacoustic properties of the bottom
3. Layer 3 - Computational scheme: physical equations used for the estimation of the propagation of sound waves; spatial, temporal and angular resolution of the calculations; sound frequencies of interest
4. Layer 4 - Field validation: comparison and calibration with field data
5. Layer 5 - Output formatting: parameters and metrics shown in the maps or necessary to correctly understand the maps, and graphical layout

As it can be understood, for each point of the above list there are several “variability factors” affecting the detailed procedure chosen for a modelling work, and hence the comparability of results from different methods. The variability is given by:

- The various methods for computing shipping distribution or density; the uncertainty about source depth, and the various methods for setting source levels of ships into the model (layer 1)
- The quality and availability of environmental inputs, and therefore the averaging methods used to overcome lacks of data or poor-quality data (layer 2)
- The existence of different acoustic models themselves, the choice of the resolution(s) for the model set up, and the choice of frequencies (layer 3)
- How field data are used for validation and calibration (layer 4)
- The way results are presented on a map: what metrics and value range are represented, the colour ramp used (layer 5)

Understood that we cannot address the whole variability described here in a unique report, we primarily present in this chapter the results obtained by using a **temporal approach** to obtain maps representing noise levels at the **two frequency bands of interest for D11C2: one-third octave bands centred at 63 Hz and 125 Hz**. Results are presented for different depths to show the variability in transmitted noise levels along the water column and thus provide elements for the discussion of how using results for assessment.

The main benchmark step is carried out by varying the manner ship source levels are set up as input data into the model and by comparing the results. The whole exercise was indeed repeated three times, each time with a different model for ship source level. Different coefficients of environmental variables are also tested in the calibration and validation phase, in order to assess the goodness of the estimations and to reduce the deviation from real data obtained via the in-situ recordings. Finally, a comparison with a **probabilistic approach** is presented for the same area.

## 5.2 Study area and period

The study area corresponds to the maritime space around the pilot project site of Cabrera, one of the three pilot site of the QUIETMED project. The coordinates of the study area were set considering the position of the recorder and the common distances at which the loss of sound energy generated by ships results in levels in the range of natural ambient noise (< 80 dB): the farthest point from the recorder deployed at Cabrera is set at about 200 km.

The study area is a square with vertices having the following coordinates (lat, lon):

- NE: 40.95, 0.618
- NW: 40.95, 5.27
- SE: 37.32, 0.618
- SW: 37.32, 5.27



Figure 15: Location of Cabrera Pilot Project in the Mediterranean Sea

The study period is the same of the Cabrera pilot, i.e. from January 19th, 2018 to February 6th, 2018 (19 days).

## 5.3 Layer 1: Shipping – Information form

### 5.3.1 Information on ships from AIS data

The AIS is a tracking system which is mandatory for every ship with tonnage above 300 tons. AIS stations continuously broadcast messages via VHF or satellite connection. These messages identify uniquely each user (vessel) and contain several parameters about the navigation: the geographical position, the speed, the heading; and about the ship: the ship type (cargo, tanker, passenger, etc.), the size, and the status (navigating or mooring). AIS data can be used to enable realistic shipping noise mapping, as they provide parameters required as input for an acoustic modelling system. For the present work, AIS messages sent by both VHF and satellite (S-AIS) were used to guarantee the best quality data were used. Data come from AIS data providers working in partnership with SINAY. Raw AIS messages were first stored in the Big Data platform of SINAY and then converted into commonly formatted matrices (CSV).

### 5.3.2 Source models

The Source Levels (SL) of ships are imperative input data to forecast the sound field created by shipping into the marine environment. Several physical phenomena can generate noise during the displacement of a ship: the cavitation effect caused by propellers, engine vibration, hull vibrations, the bow wave caused by the moving ship, etc. These phenomena generate noise at different frequency bands and with different levels. However, the cavitation effect is identified as the main cause of ship-radiated noise according to scientific literature (e.g. Leaper & Renilson, 2012) and thereby a noise source represented by a ship can be located in the position of the propeller. This point is important when discussing about the source depth, later in this document.



Figure 16: List of noise source of navigating ships

To obtain meaningful Source Levels, one option is performing complex and expensive work to measure single vessels following standard protocols (such as the ANSI/ASA S12.64-2009/Part 1 for Radiated Noise Levels<sup>2</sup>, or other protocols for direct measures of Source Levels). Therefore, approximations are commonly used to describe SL and emission spectra of vessels, and many studies have shown acceptable effectiveness (e.g. Simard et al., 2016; Veirs et al., 2016; McKenna et al., 2012). Such approximations are extrapolations (also referred to as models) derived from real data for specific vessels. The most known models are shown in Figure 16 (Cf Chapter 3).

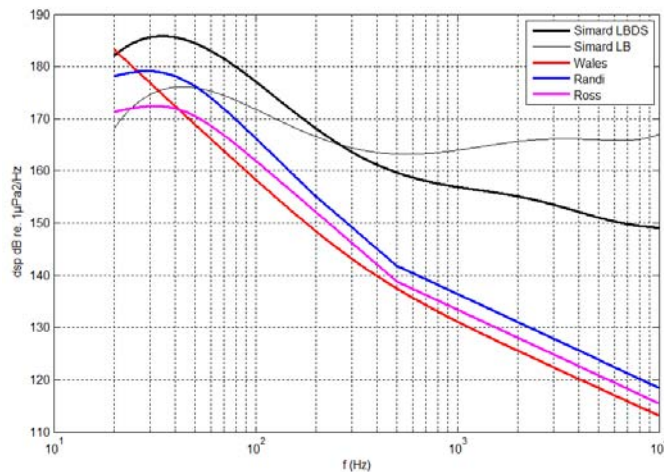


Figure 17. SL estimates according to different methods (models)

The accuracy of each source model depends on many factors, including sea state conditions, the availability of specific information about the vessel, the bathymetry, the distance of the

<sup>2</sup> “Quantities and Procedures for Description and Measurement of Underwater Sound from Ships”, Part 1: General Requirements, Approved September 30, 2009 by: American National Standards Institute, Inc.



measurements from the vessel, amongst others. Concerning the performance of each model with relationship to the present study, no previous knowledge could guide through selecting a specific source level model a priori. Subsequently, the choice of the best source level model was made a posteriori (empirically) after running the modelling algorithms with different input source data and using the field data to identify the best estimate.

### 5.3.3 Other sources properties as input data for the model: ship size, speed and depth

Concerning size and speed of ships, such data are obtained directly from the AIS data for each ship and for each AIS message received. Also, the depth of the noise source has an obvious influence on sound propagation patterns and thereby is an input data for the modelling, but it cannot be found in the AIS data and hence an approximation is again required.

The depth of the source varies according to ship type and speed, propeller position, and charge. Therefore, a depth value should ideally be assigned to each ship included in the computation. In the scientific literature, some studies say that for modelling works covering large areas (as for our case) a variation of a few meters in source depth does not influence significantly the output obtained (e.g. Gervaise et al., 2015), while in other cases the effect appear significant (see above in this document, Figure 12). Given this uncertainty, the source depth was set for all ships to 7 m following Scrimger and Heitmeyer (1991) which consider this depth as a common propeller depth for commercial ships.

## 5.4 Layer 2: Environment – Information form

Environmental data describe the propagation medium of acoustic waves and are the drivers of sound propagation. In this section, we define environmental variables, their relative effect on the propagation, and the available data sources used.

Environmental drivers are quantified through values and numerical coefficients assigned to the following parameters:

- Bathymetry
- Sound speed profile, obtained from 3-dimensional data (lat, lon, depth) of temperature and salinity
- Geoacoustic model of the bottom:
  - o number of layers (sediment layers, sub-bottom, etc.)
  - o thickness of each layer (in meters)
  - o velocity profile of sediment (also called compressional speed, m/s)
  - o density (kg/m<sup>3</sup>)
  - o attenuation of compressional waves and shear waves (dB/λ)

The selection of the coefficients depends on the availability and on the resolution of environmental data, and therefore on the assumptions made whenever necessary to overcome potential data gaps.



### 5.4.1 Bathymetry

The acoustic wave propagation in the ocean can be defined into two main phases: free propagation and interactions with frontiers and obstacles. When acoustic waves encounter the bottom, a part of the wave is transmitted into the sediment, while the other part is reflected.

The shape of the bottom is also important. Many phenomena occur during the contact of the acoustic wave with the seabed as the diffusion of waves, transmission and reflection. For this reason, the angle of incidence of the wave at the interface (water/seabed) affect the amount of energy transmitted and reflected. Therefore, the resolution of the bathymetry data is essential to obtain good quality results. In our case, over a large area covering more than 40 000 km<sup>2</sup>, a resolution of 130 m between two successive bathymetric points was considered appropriate and used as input data.

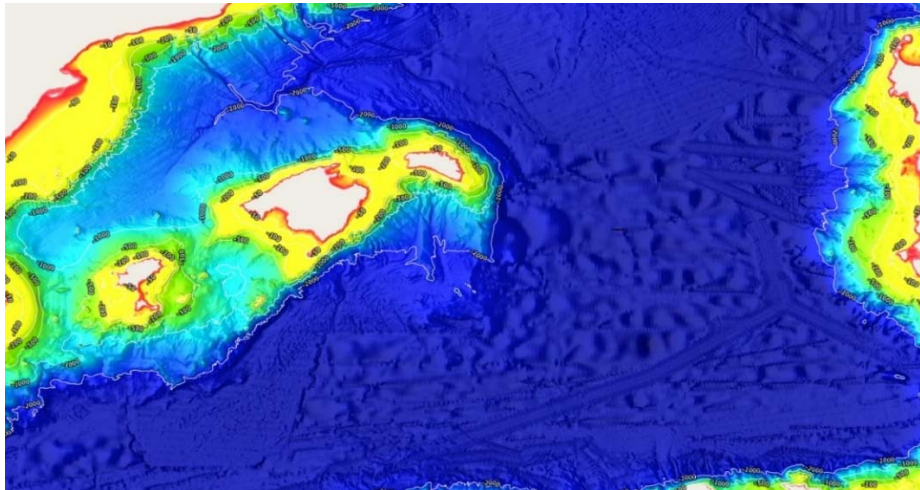


Figure 18. Bathymetric dataset used for the present work (source: EmodNet).

### 5.4.2 Sound speed profile

Due to the limitation of the propagation medium by the surface and the seafloor, the acoustic wave undergo successive reflections on the interfaces. Moreover, variations in the physical characteristics influence the speed of sound in the medium which in turn can cause deformations of the sound wave paths. Specifically, the speed of sound depends on temperature, salinity and depth and hence such parameters are necessary for calculating the velocity profile of sound in the propagation medium.

For this task, we collected the data from the available monitoring stations connected to open data platforms (such as Copernicus and EmodNet, Figure 18) during the recording period of the Cabrera pilot. The velocity profiles was then calculated for each sampling point which are shown in the figure below (Figure 19). We averaged the velocity profiles obtained for each points which runs around the measuring point in order to be able to compare correctly the recorded level with the results of the simulations.

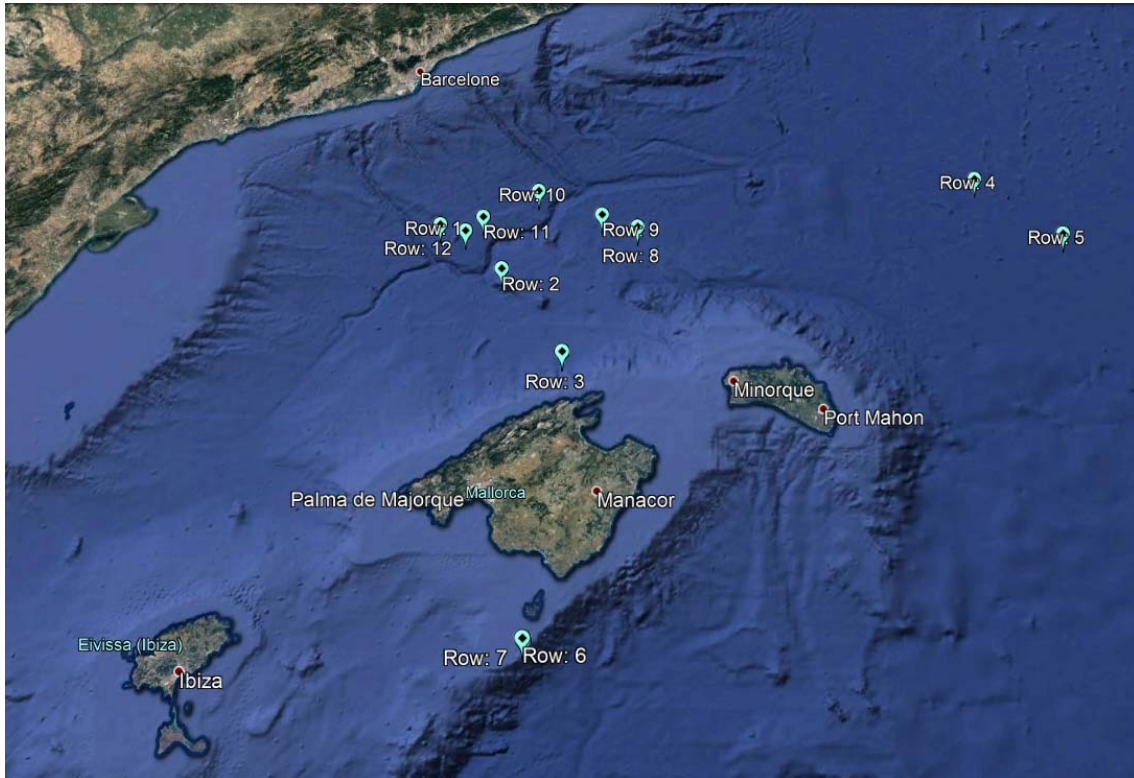


Figure 19. Sampling points for temperature and salinity.

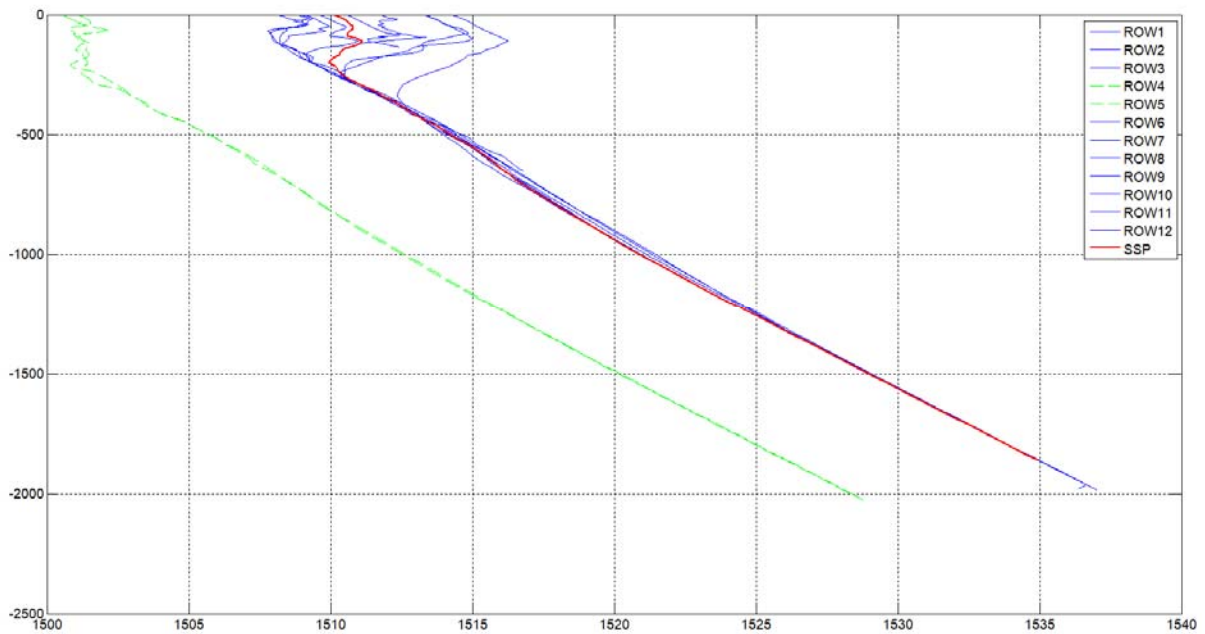


Figure 20. Sound speed profile obtained from temperature and salinity data at 12 points of measurement.

### 5.4.3 Geoacoustic properties of the bottom

The nature of the sediments have a major effect on the level of ambient noise, and is due to many phenomena occurring simultaneously: diffusion by the relief of the water-bottom interface; penetration of the sediment incident wave, sediment damping, sediment refractions and reflections, and attenuation of the P (longitudinal) and S (shear) waves. Data on the geoacoustic properties may be obtained in three ways:

- Through samples of the study site, which allows selecting the coefficient (from scientific literature) corresponding to the characteristics obtained with the samples
- With on-site calibration measurements at representative points. In this case dedicated field campaign are carried out and active controlled emissions are generated with an underwater speaker and recorded by hydrophones. In this case the propagation coefficients are derived directly from the observed transmission losses;
- Using available geological and geomorphological mapping, which allows identifying the type of sediment and thereby selecting the relative coefficients from scientific literature.

In this work we applied the last option and the geoacoustic properties are based the map produced by the SHOM and available from open data platforms (Figure 19).

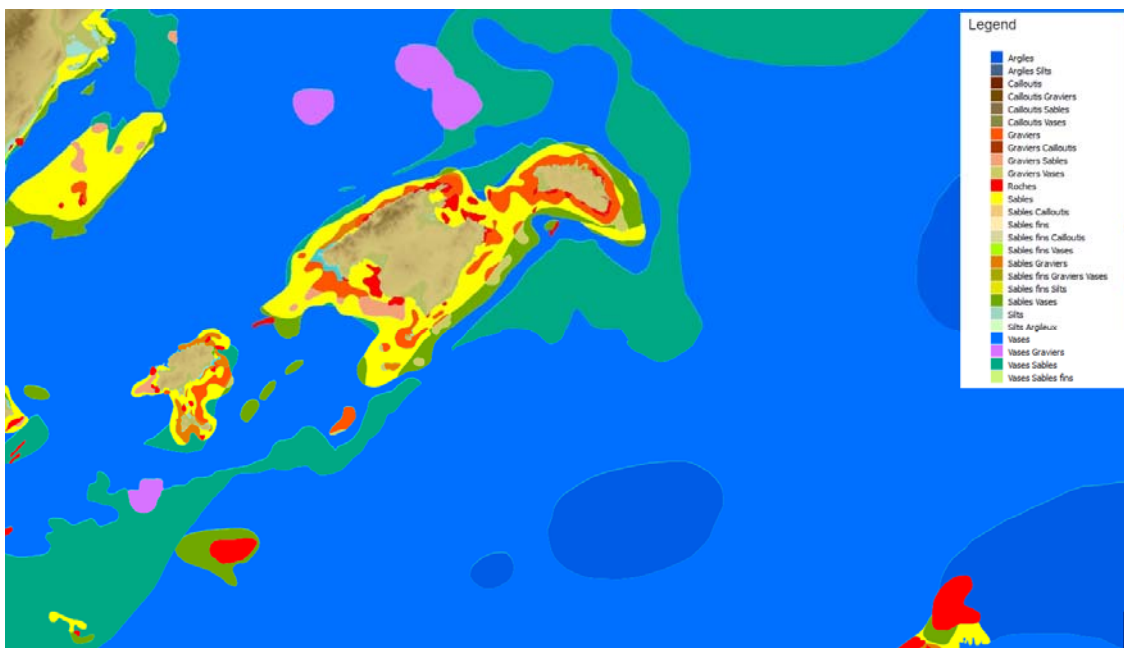


Figure 21. Seafloor geological nature (source EmodNet).

With this map, values of the acoustic properties of the Balearic Sea’s bottom can be assigned to each point of the study area. As an example, minimum and maximum values of sediment sound speed and density, as available from literature, are reported in Table 1.

Table 1. Minimum and maximum values for sound speed and density measured in sediments (Rakotonarivo, 2009)

Sediment type	Sound speed (m/s)		Density (kg/m <sup>3</sup> )	
	Min	Max	Min	Max
Coarse Sand	1780	1880	2030	2080
Medium sand	1730	1800	2000	2040
Fine sand	1645	1700	1920	1970
Very fine sand	1680	1710	1880	1940
Silty sand	1490	1660	1680	1800
Silt	1495	1620	1650	1740
Sand-silt-clay	1480	1590	1450	1620
Clay loam	1450	1550	1430	1480

We considered worth including in the model the first meters of sediments since the reflection of the bottom can have a noticeable effect, especially for shallow waters. For this exercise, we used the *medium sand* values as shown in table 1 since this sediment type covers > 80% of the studied area. We assumed that we have one layer with a gradient varying from minimum to maximum values associated to medium sand (Table 1). To test the effect of seafloor nature, we repeated the modelling exercise using extreme values. We observed that the effect is very low (some decimals of dB), likely because of the prevalence of deep waters as well as the little number of vessels located shallower waters.

Finally, mean values of the attenuation of sound waves caused by the substrate are available from the scientific literature. In Figure 21 (taken from Hamilton and Bachman, 1982), the attenuation (absorption) is shown as a function of porosity and grain size of the substrate.

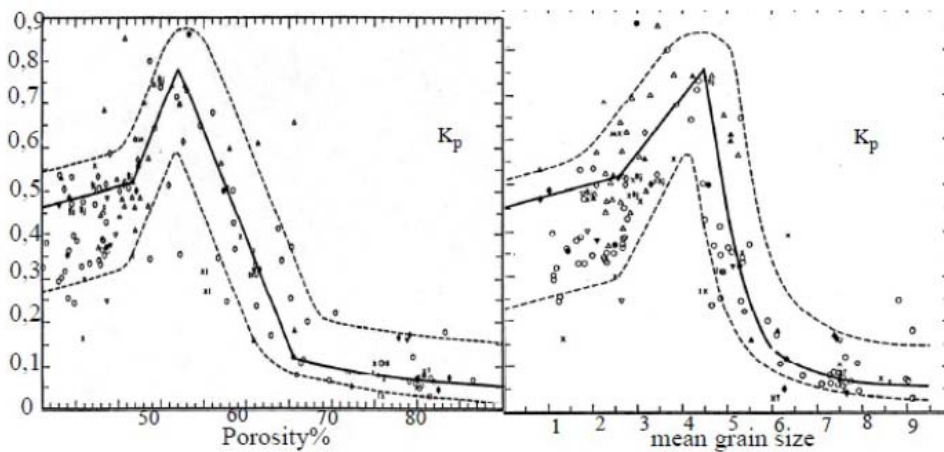


Figure 22. Absorption depending on porosity (left) and on the grain size (right).



## 5.5 Layer 3: Computation Scheme – Temporal approach with Refined Transmission Losses

The temporal approach used in this work is resumed in the following main steps:

- 1 Screenshots of ship traffic are obtained from AIS data at several instants within the study period. A traffic screenshot is an instantaneous view of the position of all ships navigating in the study area.
- 2 Noise radiated from each ship is estimated by the model. The outputs of the model are maps of received levels all over the study area. Contributions from all ships are summed up to obtain instantaneous noise screenshots. Such noise screenshots are the samples used for the subsequent statistical analysis
- 3 Statistics indicated in the technical guidance from TG-Noise are calculated: average noise levels using the arithmetic mean, the median level, and percentile levels (useful for threshold analyses)

AIS screenshots (point 1 in the list above) were taken at regular intervals of 8 hours within the study period which goes from January 19<sup>th</sup> to February 6<sup>th</sup>, 2018, meaning three screenshots per day (00:00, 08:00 and 16:00).

For the calculation of noise radiated from each ship found in a AIS screenshot (point 2 in the list above), the modelling consists in calculating the attenuation values of the waves throughout the propagation environment. Attenuation is the reduction of the acoustic intensity or the pressure level during the propagation of a sound waves in a medium between two points. It is caused by three independent phenomena:

- ✓ The loss of geometric divergence that is usually noted TL for transmission loss. It is the acoustic energy distributed in the space during the propagation of the wave;
- ✓ Absorption which is the effect due to viscosity, molecular relaxation and inter-grain friction in water or sediment. The higher the frequency of propagation, the higher the absorption of the medium.
- ✓ Interaction with obstacles (an interface such as the seabed or an object) in the water that generates a diffusion or reflection.

The procedure consists in three steps: 1) selecting the model that better describes the attenuation of sound energy according to source and environmental input parameters; 2) parametrising the model; 3) running the models. The sections hereafter detail such steps.

### 5.5.1 Selecting the best acoustic model

There are several mathematical methods (models) for calculating attenuation of acoustic waves whose performance may differ significantly in different scenarios. The principle parameters to consider for the selection of the better method are the bathymetry, the sound frequencies of interest, and whether or not variations of the environmental factors such as the sound speed profile and the geomorphology are considered to have a significant effect on the

model output. Each scenario is a combination of such parameters and the selection of the best model can be done a priori based on table 2 presented below. This table was adapted from previous review works available in the scientific literature (Etter, 2012; Farcas et al., 2016; Wang et al., 2014). A qualitative score (suitable or unsuitable) is attributed to the performance of the models in each scenario. Compared to review works mentioned above, table 2 is simplified in that a lower number of models is presented (5 in Wang et al., 2014, 4 in Etter et al., 2012), and because models are presented as suitable or unsuitable, without intermediate scoring. The scenario for the present study is described by:

- Propagation in both shallow and deep waters
- Frequency range of interest in the low frequencies (1/3 octave bands centred at 63 Hz and 125 Hz)
- Varying environmental factors:
  - o sound speed profile both vertically and horizontally
  - o complex geology and geomorphology

According to Table 2, the most appropriate propagation model appears to be the range-dependent parabolic equation (**RAM**), where range-dependent means that the environmental factors have a significant influence on propagation.

**Table 2. Theoretical effectiveness of the different modelling methods according to different combinations of input parameters: bathymetry, frequency range of interest, influence of environmental factors. RI = range-independent; RD = range-dependent.**

Models	Modelling algorithms	Applications							
		Shallow waters				Deep waters			
		Low freq		High freq		Low freq		High freq	
		RI	RD	RI	RD	RI	RD	RI	RD
Ray tracing	Bellhop (Porter & Liu)								
Normal modes	Kraken (Porter)								
Parabolic equation	RAM (Collins)								

Suitable
  Not suitable

### 5.5.2 Model set up

The model is set up by specifying a number of parameters:

- ✓ Angular Resolution. The model calculates the sound waves propagation in the 360 degrees and an angular resolution need to be specified. This greatly affects the resolution of the results and the computation time. In this study we set the angular resolution at 0.5 degrees (which is a very high resolution) thanks to the significant computing capacity of the modelling system developed at SINAY.

- ✓ Propagation distance from the source in the horizontal plane is set at 200 km. At this distance, the loss of acoustic energy results in noise levels which are comparable to values commonly considered in the range of natural ambient noise. This means that the model calculates the transmission losses until 200 km from the noise source.
- ✓ Horizontal resolution (spatial resolution for the lon/lat plane). The horizontal resolution was set to 100 meters. Considering the previous parameters (propagation distance 200 km and angular resolution 0.5 degrees), this means that the model estimate a received noise level every 100 m until the maximum distance, resulting in 2 000 estimations, multiplied for the total number of angles used ( $360/0.5 = 720$ ). The result is 1 440 000 estimations for a single horizontal plane.
- ✓ Vertical resolution (spatial resolution for the distance/depth plane). The vertical resolution is set to 4 m. Here, the maximum propagation distance in the vertical plane is given by the depth of the bottom and the number of estimations a function of the depth.
- ✓ Number of frequencies for each source. Each source has several transmission frequencies. The frequencies of interest for the D11C2 are the third-octave frequency bands centred at 63 Hz et 125 Hz. The computation is done for such two third-octaves, separately.

### 5.5.3 Running the model over the study period

For each AIS screenshot, the procedure described above is repeated a number of times equal to the sample size (57) to obtain as many noise screenshots, for each depth and source model tested. Subsequently, the arithmetic mean and the percentiles are calculated.

## 5.6 Layer 4: Calibration and validation

Results from field data were kindly made available by UPV from the recorder deployed in Cabrera. This allowed a first comparison with levels estimated by our model. The comparison work was carried out for both low and high noise periods.

As mentioned above, we tested 3 different source emission models and we detected that the lowest difference (+5dB) was compared to measurements was found in the output obtained with SIMARD source emission model (See Figure 16). Such difference corresponds to a good correlation. Instead, for Randi and Ross models, the output resulted in a difference up to 20 dB.

The key message here is that the comparison of estimates with recordings helped us to designate the source model (Simard) that generated the closest output to observed noise levels.

Refined results may be obtained in the following ways:



- ✓ Studying geo-acoustic parameters related to the exact nature of sediments instead of approximations as used in the present study
- ✓ Improving the quality and availability of temperature and salinity data
- ✓ Improving the way AIS data are used, correcting incomplete or erroneous data (in the present study such incomplete or erroneous data were omitted)
- ✓ Further increasing the spatial resolution (implies increasing computational time and costs)

## 5.7 Layer 5: Results, formatting and displaying

We produced 509 instantaneous maps (noise screenshots):

Table 3. Summary of results for noise screenshots.

Third-octave band	Depth layer	Source model	# maps produced (8h time interval)
63 Hz	12 m	Simard	57
63 Hz	100 m	Simard	57
63 Hz	100 m	Randi	57
63 Hz	100 m	Ross	57
125 Hz	12 m	Simard	57
125 Hz	100 m	Simard	54
125 Hz	200 m	Simard	57
125 Hz	12 m	Randi	56
125 Hz	12 m	Ross	57

And 27 indicator maps:

Table 4. Summary of results for indicator maps, i.e. maps showing statistics indicated in guidance from TG-Noise.  
\* the number of maps reflects the number of statistics calculated: arithmetic mean and percentiles 50 and 95.

Third-octave band	Depth layer	Source model	# maps produced*
63 Hz	12 m	Simard	3
63 Hz	100 m	Simard	3
63 Hz	100 m	Randi	3
63 Hz	100 m	Ross	3
125 Hz	12 m	Simard	3
125 Hz	12 m	Randi	3
125 Hz	12 m	Ross	3
125 Hz	100 m	Simard	3
125 Hz	200 m	Simard	3

The two third-octave bands centred at 63 Hz and 125 Hz are clearly indicated in available guidance as the focus for the monitoring of anthropogenic noise in the marine environment. Further, the reason for testing different source models (Simard, Ross and Randi) derives from the absence of *a priori* knowledge on emission levels and spectra of ships in the study area (see 4.3.2). Therefore, estimates obtained with different source models were used for comparing with field results and finding the computation scheme resulting in the best estimates for the area. Finally, concerning the depth layer, the available guidance on D11C2

does not indicate precisely what depth to consider for the monitoring and, more in general, how to consider the variation of noise levels with depth for monitoring and assessment purposes. Therefore, depth layers were selected for displaying results based on the reasons described in the following table:

Depth	Reason	Usefulness
12 m	To explore surface noise levels, where noise sensitive species like cetaceans spend most of their (non foraging) time	Assessment
100 m	To compare model outputs with recordings (the recorder was deployed at 100 m depth)	Calibration/Validation, and assessment
200 m	To get an insight about noise levels in deeper areas.	Assessment

Maps show received levels in dB re 1µPa. The scale of the color bar is between 40 and 140 dB. The blue and light blue areas range between 40 and 80 dB. This range cover the levels generally considered natural ambient noise. All other areas present shipping noise contribution, which increases from green to red areas.

### 5.7.1 Noise screenshots in the Balearics

In this section we show noise screenshot maps, i.e. the samples used for the subsequent statistical analysis. Concerning the 509 noise screenshots produced during this study, we show in this section a selection of indicative examples pointing out relevant acoustic phenomena and highlighting the effect of varying parameters on the output.

The maps of Figure 22 compare the estimations obtained exploring different source models and different depth layers. For a single instant (January 21<sup>st</sup> 2018 at 08:00), and for the one-third octave bands centred at 125 Hz, the figure shows the variability of results obtained using three source models (Simard, Randi, Ross) at the same depth (left pictures), and with the same source model (Simard) but at three different depth layers (12 m, 100 m and 200 m).

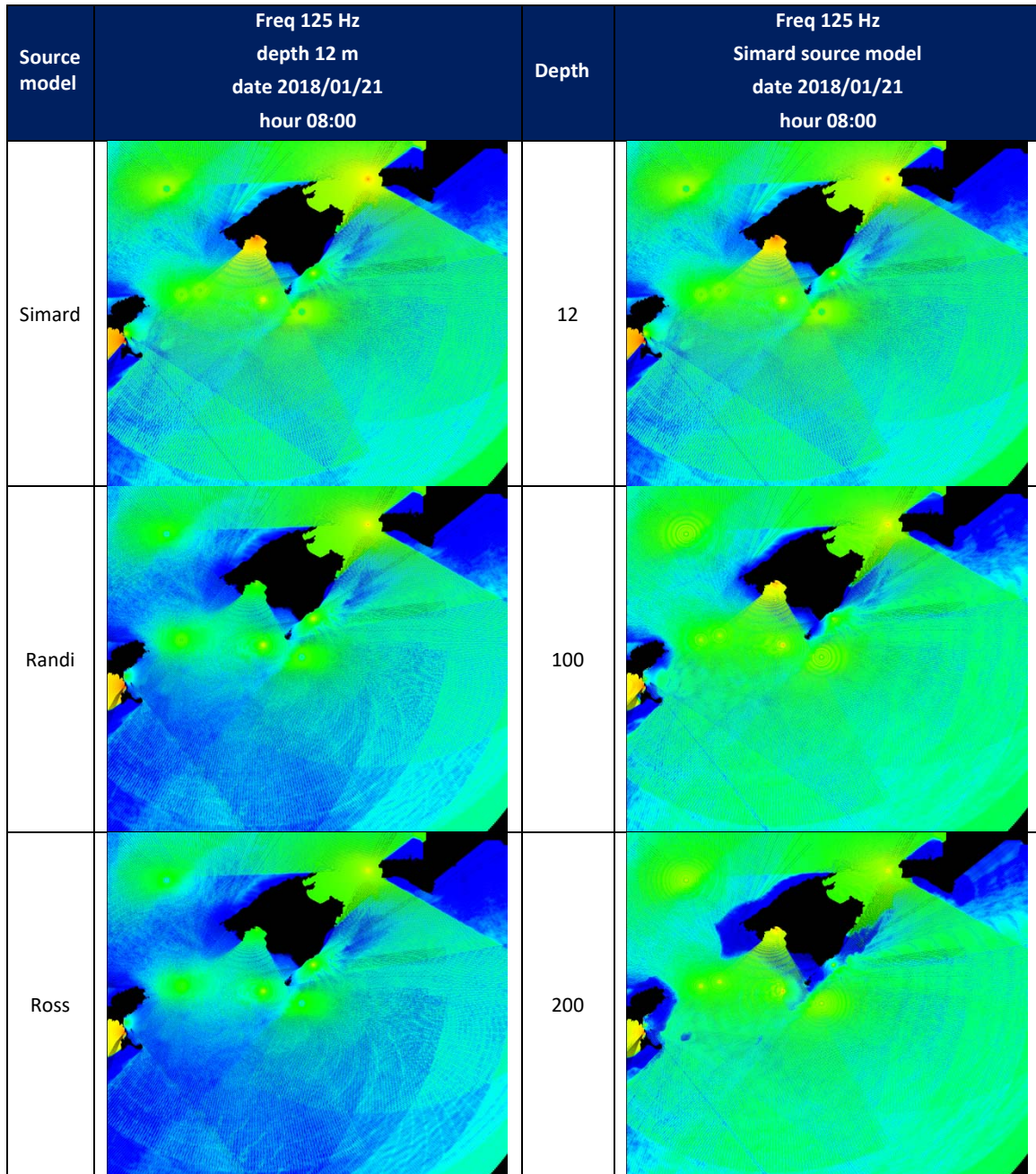


Figure 23. Variability in results estimated with varying parameters for the same noise screenshot. Left pictures focus on the effect of the source model. Right pictures on the effect of bathymetry. The first row shows the same twice, as to better describe the great variability, and hence the sensitivity of the choice for assessment purposes.

From Figure 22 it is possible to appreciate that sound wave propagation often follows a sinusoidal path in the vertical plane (depth/distance plane). This phenomenon may occur when particular oceanographic characteristics exist and result in areas known as convergence zones. As the maps are shown in the horizontal plane (lat/lon), this phenomenon is recognised thanks to the concentric circles that are visible in the pictures and having their centre in the position of the noise sources (i.e. the vessels). These maps show that the noise generated by a single ship may be heard at tens or even hundreds of kilometres. In left pictures, the effect of

different source models as input data is evident and the results present considerable differences.

Considering right pictures in Figure 22, estimated noise levels close to vessels are generally decreasing with depth, while this may not be true in the far field. The distribution of energy does not follow indeed the same distribution at all depths, this is due to different phenomena such as the reflections from the bottom and surface and the variation of the sound speed profile in the water column which concentrates the energy of the acoustic waves in the depth level with the minimum sound speed value. According to the profile (see Figure 18) this minimum is found in the first tenths of a meter. A synergy of such phenomena may result in increasing noise levels far from the source and at increasing depth (e.g. in the SE area of Menorca) where values do not exceed 65 dB re 1 $\mu$ Pa at 12 m while reaching 90 dB re 1 $\mu$ Pa at 200 m. Finally, we can appreciate the effect of the bathymetric attenuation on acoustic wave propagation along with depth, particularly close to the islands.

Globally, the maximum estimated SPL value among these examples was 189 dB re 1 $\mu$ Pa, for the map at 12 m depth, using the Simard source model.

### 5.7.2 D11C2 Indicators: average noise levels and other statistics

In this part we present the indicators recommended in the guidance from TG-Noise concerning continuous noise (D11C2). It should be considered that the Commission Decision 2017/848 states that the monitoring should be done per quarter or per month, and that, in line with the initial project planning, the period of the Cabrera pilot project (as the other pilot projects) is lower than the requirement (3 weeks in the case of Cabrera).

The first indicator is the **arithmetic mean** calculated over all the samples  $N = 57$ , for each depth layer), where these are the noise screenshots obtained through repeated modelling (Cf. section 4.5). Further, we calculated two indicators in percentiles. Here we use the definition given by the international standard ISO 1996-1: 2003 (E), defining percentiles as exceedance levels. According to this definition, the percentile  $N$  is the noise level exceeded for  $N\%$  of the time of the study period. Therefore, percentile levels show, for each point in the study area, how long a noise level is exceeded as a percentage of the study period. Such indicators are the **50% Exceedance Level** (which is also the median level) and the **5% Exceedance Level** (meaning the noise levels exceeded during 5% of the study period, which represent the highest levels estimated).

The three indicators are shown in Figure 23 for the 1/3 octave bands centered at 63 Hz at 12 m and 100 m. For the 1/3 octave band centred at 125 Hz, indicators are shown in Figure 24 for three depth layers: 12 m, 100 m and 200 m.



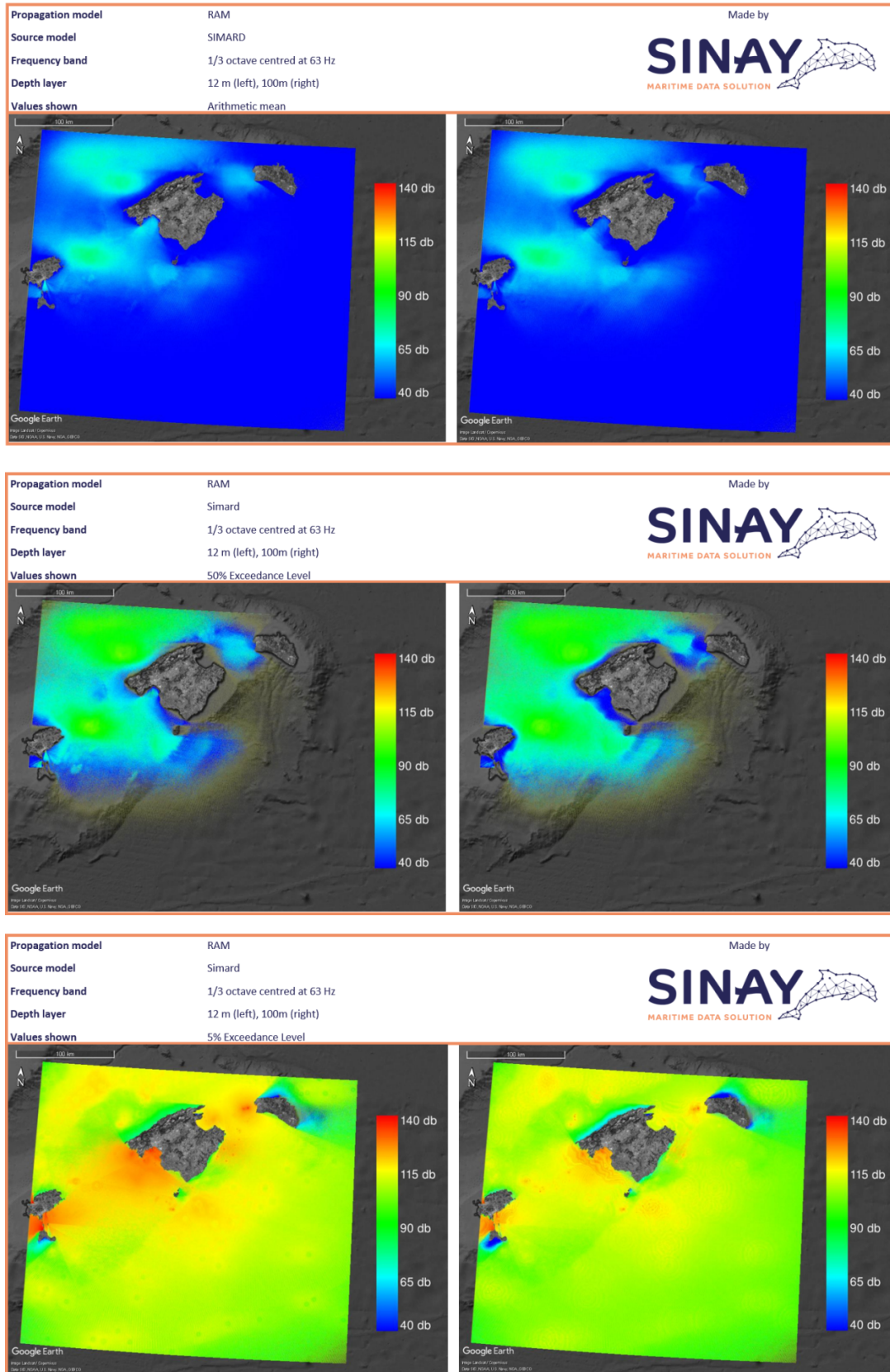


Figure 24. SPL statistics in the Balearics for the 1/3 octave band centred at 63 Hz: average (arithmetic mean), median (50% Exceedance level) and loudest noise (5% Exceedance levels) at two depth layers.

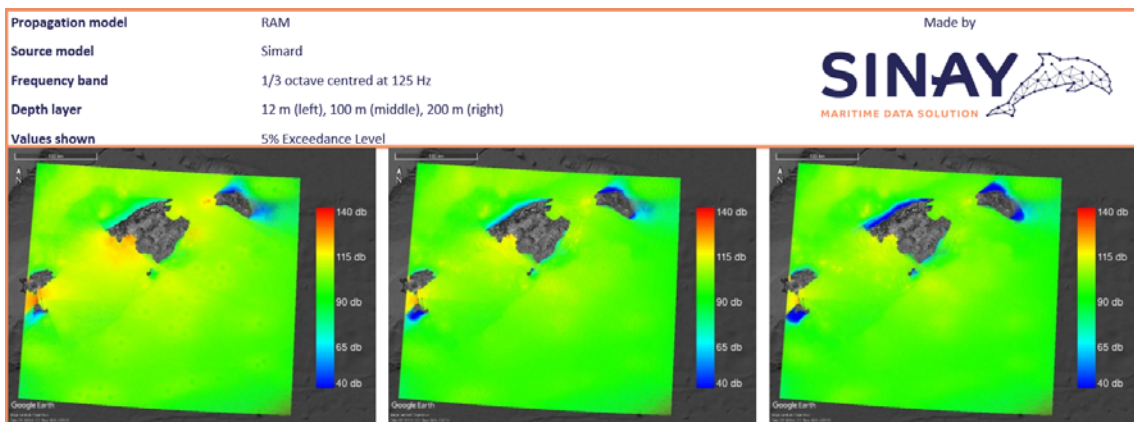
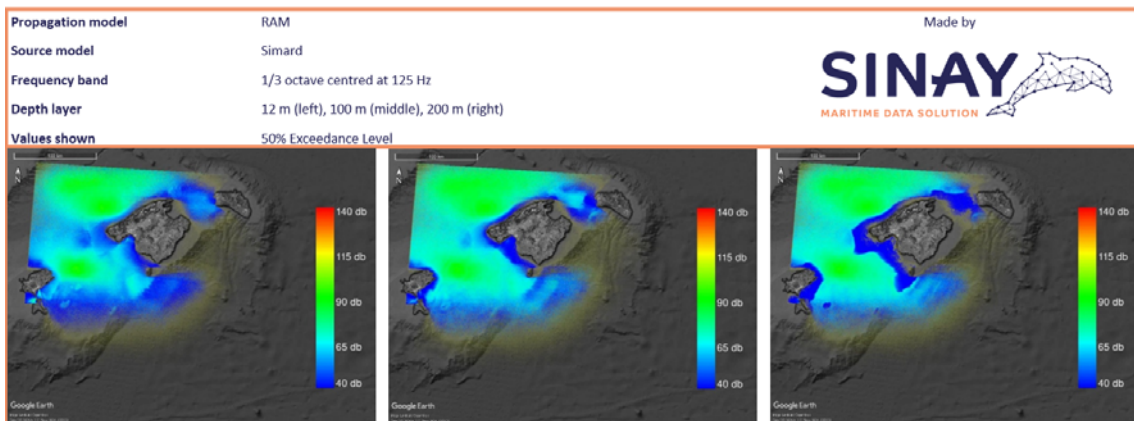
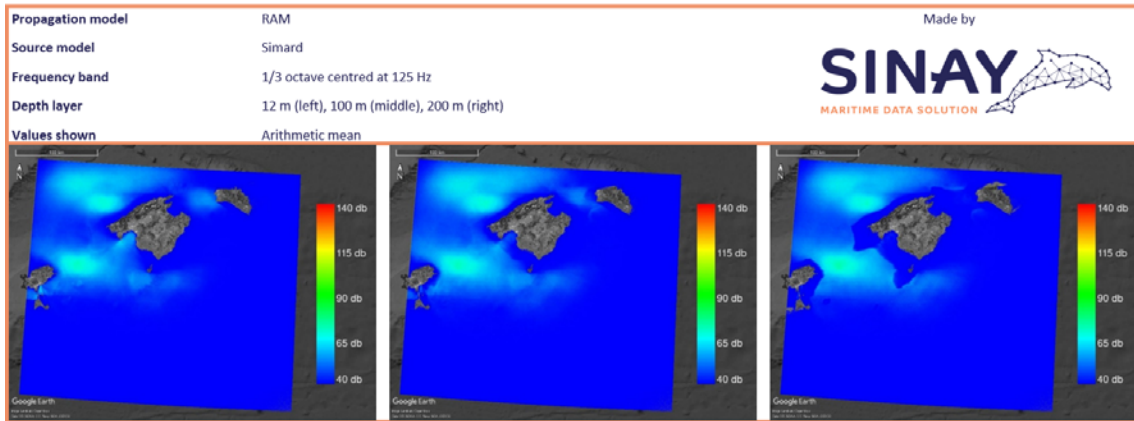


Figure 25. Noise statistics in the Balearics: average (arithmetic mean), median (50% Exceedance level) and loudest noise (5% Exceedance levels) at three depth layers.

These maps can be read as follows, for example concerning Figure 23 : in the SW area of the island of Mallorca and between the islands of Ibiza and Formentera the model estimated more than 140 dB re 1 $\mu$ Pa for a proportion of time equal to 5% of the study period (1/3 octave band centred at 63 Hz). On the other hand, the model estimated that in the NW part of the study area and between Mallorca and Ibiza, for the half of the study period (50% of time) there are levels above 90 dB re 1 $\mu$ Pa for both 1/3 octave bands. Of course this can be read on the other way round, that is to say that for the other half of the study period levels are below 90 dB. The maps representing average noise (arithmetic mean) show most of the study area with levels in

the range of natural ambient noise. Average noise is under 100 dB re 1 $\mu$ Pa throughout the study area.

The results show that the noise level in the third octave of 63 Hz is generally higher than that of 125 Hz. This is related to the nature of the noise sources (ships).

### 5.7.3 Comparison of different setups

Finally, we present maps showing different results obtained with the same computational scheme but different input data. In particular, maps of Figure 25 show the effect of using different source emission levels and spectra (i.e. source models) on estimated noise levels in the study area.

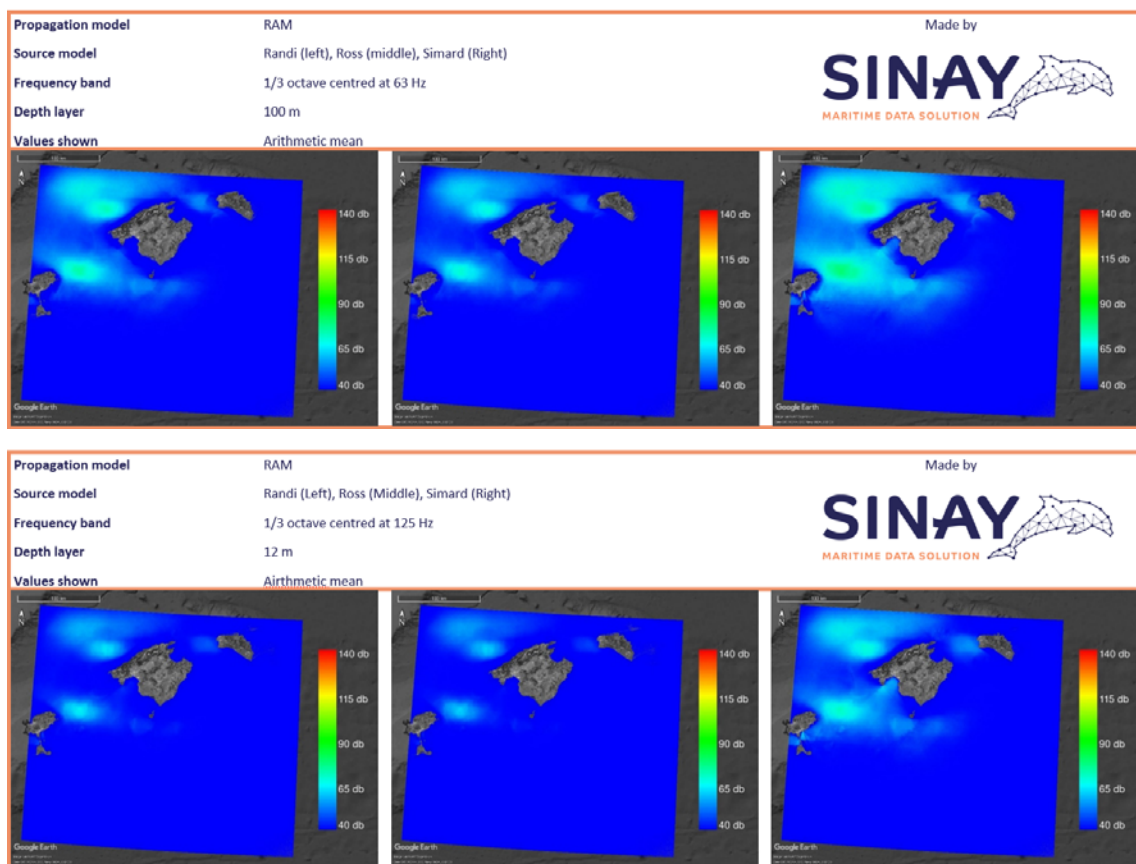


Figure 26. Effect of source models on estimated noise levels.

As described in section 4.6 (calibration and validation), the source model yielding the best estimates compared to field results is the Simard source model. At 100 depth, the maximum detected deviation is + 5 dB which is considered a good correlation.



#### 5.7.4 Comparison with a different modelling approach: Noise maps in the Balearics using probabilistic modelling

In this part we used the model developed by SHOM (Cabot, Le Courtois et al, 2016). This model is reported in literature and allows the prediction of the traffic noise in the sea. It has been validated using several opportunistic monitoring. In addition, it provides an averaged received level and a standard deviation, computed using a linear model of uncertainties; the standard deviation is interpreted as a quality factor on the estimates. This probabilistic approach provides results that complete those obtained with the temporal approach described in the previous section and may reduce the uncertainty.

The general structure is the same than described in chapter 4, i.e. the model is built specifying five layers of information (shipping data, environmental data, computational scheme, validation procedure, result formatting). The major change compared to the temporal approach is the computational scheme: instead of using ships as noise sources in their true locations (point data) to compute transmission loss, the shipping density is computed over a grid in terms of hours of navigation per grid cells and then the transmission loss is applied. This section is focused on the comparison of results, and therefore only a summary of the implementation procedure is reported here, whereas more details are found in Le Courtois et al, 2016.

Data and parametrisation of the model is briefly reported hereafter:

- Input data concern the month of January 2017
- Horizontal resolution: 1 minute in latitude and longitude
- Ship data : the Automatic Identification System (AIS) data from Lloyd's (VHF and satellite) to obtain the traffic density during the study period
- Frequencies: those recommended for D11C2, i.e. two third-octaves frequency bands centred at 63 Hz and 125 Hz
- Depths displayed: the depths 12 m is shown to model the effect of noise on the surface and 100 m for comparison between the model outputs and the recordings.

Results are shown in Figure 26. These maps show the noise generated by each ship present in the study area in dB re 1  $\mu$ Pa. The results appear similar than those in the previous sections (Cf. 4.7.2). The main structures and hotspots can be found on both the probabilistic and the temporal approach: they depend mainly on the traffic activities and seabed composition.

However, although many input data are the same for the two approaches, it is evident here that the comparability is qualitative, and many parameters need to be harmonised to get fully comparable results, including in quantitative terms: the horizontal and vertical resolution, the size of the study area, amongst others.

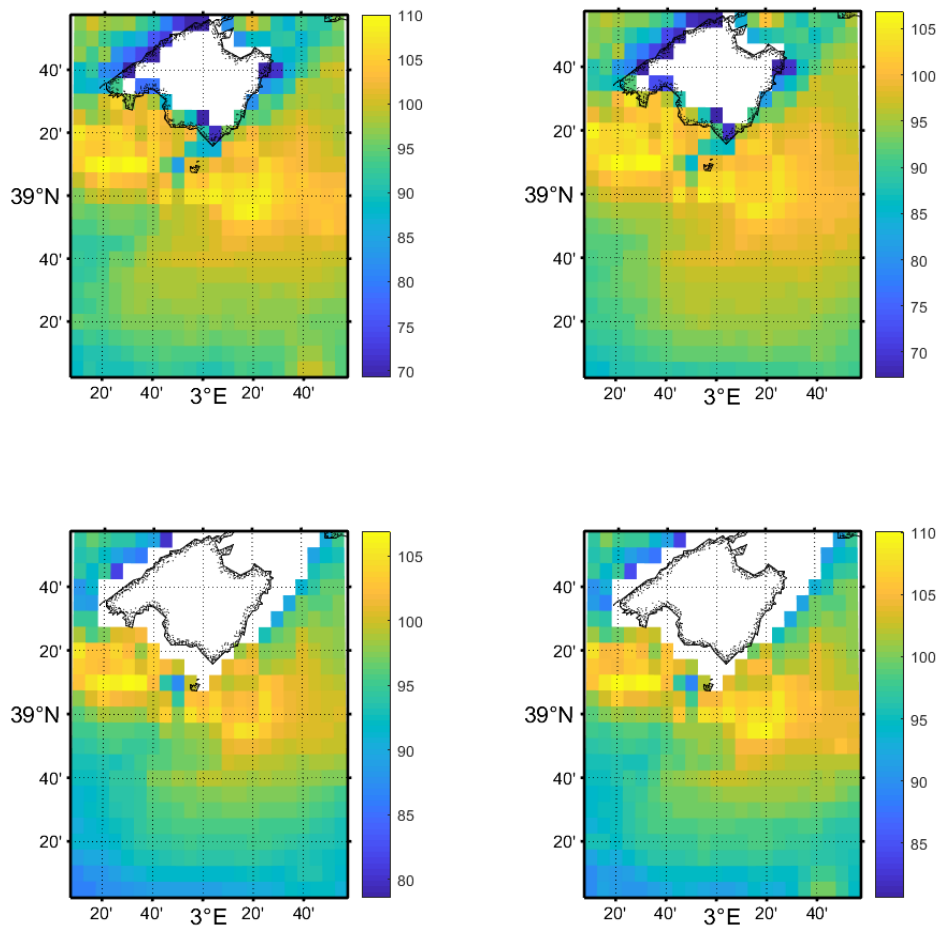


Figure 27. Sound pressure levels (SPL) from shipping activities for the month of January 2017 (in dB re 1  $\mu$ Pa) for the one-third octave bands centred at 63 Hz (left) and 125 Hz (right). Top panel: 12m depth. Bottom panel: 100m depth.

Other comparisons may be presented from different setups and approaches, resulting in a number of estimates ranging between a minimum and a maximum value. As such, and considering all the information presented in chapter 4, the main conclusions here appear to be the following:

- An identity card of the global modelling picture is necessary not only for a better understanding and interpretation of results, but also for comparing results from different marine regions or subregions (which very likely will be obtained by different institutions)
- The great variability in noise modelling schemes, as highlighted and confirmed in this report, may be an issue if we want to work with absolute values and, for example, setting unique values as thresholds for management purposes
- On the other hand, from a qualitative point of view, all model setups and results presented here allow locating areas of higher noise. This may be sufficient in terms of management (but sufficient evidence of negative impact on the marine environment should support management measures)

## 6 Conclusions, perspectives, recommendations

Because of the above pitfalls, modelling results are more of qualitative rather than quantitative value, at least for the present. Nevertheless, even these qualitative conclusions can be of great importance for the meaningful design and conduct of noise measurements. For example the dependence of the noise field with depth in summer, as demonstrated in [Skarsoulis et al. 2017], is a significant feature that should be taken into account in the design of noise monitoring campaigns.

As already mentioned, there is hope that in the future more detailed ship characteristics related to acoustic emission will become available, based on the increasing interest by the IMO members in addressing noise pollution. This will be a great step toward the increase of reliability of the noise distributions predicted from modelling. Further, three key-components should be addressed in the future:

- ✓ Metadata: the definition of a sort of *identity card* of the modelling scheme used (model ID) to allow transparency, repeatability, and reproducibility of shipping noise mapping. This model ID would allow comparing results from different modelling schemes and better distinguishing the variability due to natural factors from artefacts of the experimental methodology used. Such an identity card should support a transparent understanding of predictions by providing the complete range of information and data associated to modelling results, including: metadata on input data sources, a clear indication of the transmission loss algorithm used, and all the settings (vertical, horizontal, and angular resolution, frequency bands, statistics, output formatting, etc) used to produce and display maps of shipping noise
- ✓ Sensitivity analysis: The proposition of a set of metrics to assess the overall accuracy of the modelling approaches, to account for the natural variability of inputs (ex. source level of ships, sound speed profile), for the possible knowledge gaps concerning environmental input data (e.g., sea bottom characteristics and their geo-acoustic features), and for the sensitivity to settings of the modelling procedure.
- ✓ Calibration: The proposition of a set of metrics to compare theoretical model outputs with *in-situ* measurements, and methods to calibrate theoretical output (ex. level adjustment, passive inversion, data assimilation, etc.).

## 7 Literature

1. Ainslie M.A., Heaney, K.L., Binnerts, B., Sertlek, H., Theobald, P.D., and Pangerc T. 2014. Use of Sound Maps for monitoring GES: Examples and way ahead TNO 2014 R11167
2. *American National Standard*. (2009). Quantities and Procedures for Description and Measurement of Underwater Sound from Ships – Part 1 :General Requirements. *American National Standard, ANSI/ASA S, 34*. [http://doi.org/10.1016/0003-6870\(91\)90314-8](http://doi.org/10.1016/0003-6870(91)90314-8)
3. Andrew, R.K., Howe, B.M., Mercer, J. a., Dzieciuch, M. a., 2002. Ocean ambient sound: Comparing the 1960s with the 1990s for a receiver off the California coast. *Acoust. Res. Lett. Online* 3, 65. doi:10.1121/1.1461915
4. Aulanier, F., Simard, Y., Roy, N., Gervaise, C., & Bandet, M. (2016). Spatial-temporal exposure of blue whale habitats to shipping noise in the St Lawrence system., Advisory Secretariat, Report 2016/090.
5. Aulanier, F., Simard, Y., Roy, N., Gervaise, C., & Bandet, M. (2017). Effects of shipping on marine acoustic habitats in Canadian Arctic estimated via probabilistic modeling and mapping. *Marine Pollution Bulletin*, 125(1–2), 115–131. <https://doi.org/10.1016/j.marpolbul.2017.08.002>
6. Bassett, C., Polagye, B., Holt, M., and Thomson, J. A Vessel Noise Budget for Admiralty Inlet, Puget Sound, Washington (USA), *J. Acoust. Soc. Am.*, vol. 132, pp. 3706–3719, 2012.
7. Baudin, E.B., and Mumm, H.M. 2015. Guidelines for regulation on UW noise from commercial shipping. SONIC deliverable 5.4, Rev. 4.3. European Commission FP7-GRANT AGREEMENT NO. 314227
8. Borsani, J.F., Faulkner, R., Merchant, N.D. 2012: Impacts of noise and use of propagation models to predict the recipient side of noise, Final Report, ENV.D.2/FRA/2012/0025
9. Colin, M. E., Ainslie, M. A., Binnerts, B., de Jong, C. A., Karasalo, I., Östberg, M., ... & Clorennec, D. (2015). Definition and results of test cases for shipping sound maps (pp. 1-9). IEEE.
10. Collins, M.D, 1993, A split-step Padé solution for the parabolic equation method, *J. Acoust. Soc. Am.* 94(4) : 1736 – 1742
11. Dahl, P.H., Miller, J.H., Cato, D.H., Andrew, R.K., 2007. Underwater ambient noise. *Acoust. Today* 23–33.
12. Erbe, C., MacGillivray, A., and Williams, R. 2012. Mapping cumulative noise from shipping to inform marine spatial planning. *J. Acoust. Soc. Am.* 132(5): EL423-EL428.
13. Erbe, C., Williams, R., Sandilands, D., and Ashe, E. 2014. Identifying modeled ship noise hotspots for marine mammals of Canada's Pacific region. *PLOS ONE* 9(3): e89820.
14. Etter, P.C., 2012. Advanced applications for underwater acoustic modeling. *Adv. Acoust. Vib.* 2012. doi:10.1155/2012/214839.
15. Farcas, A., Thompson, P.M., Merchant, N.D., 2016. Underwater noise modelling for environmental impact assessment. *Environ. Impact Assess. Rev.* 57, 114–122.

- doi:10.1016/j.eiar.2015.11.012.
16. Folegot, T., Gervaise, C., Stephan, Y., Clorennec, D., & Kinda, B. (2012, April). Now casting Anthropogenic Ocean Noise in High Pressure Areas. In *Acoustics 2012* (pp. n-c).
  17. Frankel, A. S., Ellison, W. T., & Buchanan, J. (2002, October). Application of the Acoustic Integration Model (AIM) to predict and minimize environmental impacts. In *OCEANS'02 MTS/IEEE* (Vol. 3, pp. 1438-1443). IEEE.
  18. Gervaise, C., Aulanier, F., Simard, Y., & Roy, N. (2015). Mapping probability of shipping sound exposure level, 137(May), 429–435. <https://doi.org/10.1121/1.4921673>
  19. Gisiner, R., Harper, S., Livingston, E., & Simmen, J. (2006). Effects of Sound on the Marine Environment (ESME): An underwater noise risk model. *IEEE Journal of Oceanic Engineering*, 31(1), 4–7. <https://doi.org/10.1109/JOE.2006.872212>
  20. Hildebrand, J.A., 2009. Anthropogenic and natural sources of ambient noise in the ocean. *Mar. Ecol. Prog. Ser.* 395, 5–20. doi:10.3354/meps08353.
  21. Jensen, F. B., Kuperman, W. A., Porter, M. B., & Schmidt, H. (2000). *Computational ocean acoustics*. Springer Science & Business Media.
  22. Kinda, G. B., Le Courtois, F., & Stéphan, Y. (2017). Ambient noise dynamics in a heavy shipping area. *Marine Pollution Bulletin*, 124(1), 535–546.
  23. Leaper, R.C., Renilson, M.R., 2012. A review of practical methods for reducing underwater noise pollution from large commercial vessels. *Int. J. Marit. Eng.* 154, A79–A88. doi:10.3940/rina.ijme.2012.a2.227
  24. Le Courtois, F., Kinda, G.B., Stéphan, Y., Boutonnier, J.-M., Sarzeaud, O., 2016. *Statistical Ambient Noise Maps from Traffic at World and Basin Scales*. (Cambridge, UK).
  25. Maglio, A., Soares, C., Bouzidi, M., Zabel, F., Souami, Y., & Pavan, G. (2015). Mapping shipping noise in the Pelagos Sanctuary (French part) through acoustic modelling to assess potential impacts on marine mammals. *Sci. Rep. Port-Cros Natl. Park*, 29, 167–185.
  26. Maglio, A., Drira, A., Fossati, C., & Pavan, G. (2017). Modelli di previsione della propagazione sonora in ambiente marino per il monitoraggio del rumore subacqueo e del suo impatto sui cetacei. *Associazione Italiana Di Acustica*, 20–21.
  27. McKenna, M. F., Ross, D., Wiggins, S. M., & Hildebrand, J. A. (2012). Underwater radiated noise from modern commercial ships. *The Journal of the Acoustical Society of America*, 131(1), 92–103. <https://doi.org/10.1121/1.3664100>
  28. Merchant, N. D., Brookes, K. L., Faulkner, R. C., Bicknell, A. W. J., Godley, B. J., & Witt, M. J. (2016). Underwater noise levels in UK waters. *Scientific Reports*, 6(1), 36942.
  29. Merchant, N. D., Witt, M. J., Blondel, P., Godley, B. J., & Smith, G. H. (2012). Assessing sound exposure from shipping in coastal waters using a single hydrophone and Automatic Identification System (AIS) data. *Marine Pollution Bulletin*, 64(7), 1320–1329. <https://doi.org/10.1016/j.marpolbul.2012.05.004>
  30. Mikhalevsky, P.N. and Dyer, I., Approximations to Distant Shipping Noise Statistics. *J Acoust Soc Am.*, vol. 63, pp. 732-738, 1978.
  31. Porter, M. B., & Bucker, H. P. (1987). Gaussian beam tracing for computing ocean acoustic fields. *The Journal of the Acoustical Society of America*, 82 (4), 1349-1359.

32. Porter, M., & Henderson, L. (2013, June). Global ocean soundscapes. In Proceedings of Meetings on Acoustics ICA2013 (Vol. 19, No. 1, p. 010050). ASA.
33. Redfern, J.V., Hatch, L.T., Caldwell, C., DeAngelis, M.L., Gedamke, J., Hastings, S., Henderson, L., McKenna, M.F., Moore, T.J., and Porter, M.B. 2017. Assessing the risk of chronic shipping noise to baleen whales off Southern California, USA. *Endangered Species Research* 32: 153-167.
34. Ross, D. (1976). *Mechanics of underwater noise*, Pergamon, New York, 1976
35. SHOM, F. L. C., Kinda, F. G., HOM, S., HOM, J. B., Stéphan, F. Y., & ECTIA, O. S. Statistical ambient noise maps from traffic at world and basin scales
36. Siderius, M., and Porter, M.B. 2006. Modeling techniques for marine-mammal risk assessment. *IEEE J. Oceanic Eng.* 31(1): 49-60.
37. Simard, Y., Roy, N., Cedric, G., & Giard, S. (2016). Analysis and modeling of 255 source levels of merchant ships from an acoustic observatory along St. Lawrence Seaway. *J. Acoust. Soc. Am.*, 140(3), 2002–2018. <https://doi.org/10.1121/1.4962557>
38. Skarsoulis, E.K., Piperakis, G.S., Orfanakis, E. and Papadakis, P., Prediction of shipping noise in the Eastern Mediterranean Sea, *Proc. Internoise 2016*, pp. 329-336, Hamburg, 2016.
39. Skarsoulis, E.K., Piperakis, G.S., Orfanakis, E., Papadakis, P., and Taroudakis M., Modelling of Underwater Noise Due to Ship Traffic in the Eastern Mediterranean Sea, In proceedings of the 4th Underwater Acoustics Conference and Exhibition (UACE2017), pp. 889-896, (2017).
40. Taroudakis, M.I and Nikolaidis N.X., A Simplified Model for the Estimation of the Traffic Noise in Shallow Water, *Technika Chronika – Scientific Edition B*, vol. 9, pp. 47-72, 1989.
41. Taroudakis, M.I. A Study of the Influence of the Environmental Parameters on the Traffic Noise in the Sea, *Colloque De Physique*, No 2, Supplement, Tome 51, Pp C2.1001-C2.1004, 1990
42. Van der Graaf, A.J. Ainslie, M.A. André, M., Brensing, K., Dalen, J., Dekeling, R.P.A., Robinson, S., Tasker, M.L., Thomsen, F. and Werner, S. *European Marine Strategy Framework Directive - Good Environmental Status (MSFD GES): Report of the Technical Subgroup on Underwater noise and other forms of energy*, 2012.
43. Veirs, S., Veirs, V., & Wood, J. D. (2016). Ship noise extends to frequencies used for echolocation by endangered killer whales. *PeerJ*, 4, e1657. <https://doi.org/10.7717/peerj.1657>
44. Viola, S., Grammauta, R., Sciacca, V., Bellia, G., Beranzoli, L., Buscaino, G., ... Riccobene, G. (2017). Continuous monitoring of noise levels in the Gulf of Catania (Ionian Sea). Study of correlation with ship traffic. *Marine Pollution Bulletin*, 121(1–2), 97–103.
45. Wagstaff, R. A. (1973). RANDI : research ambient noise directionality model.
46. Wales, S. C., & Heitmeyer, R. M. (2002). An ensemble source spectra model for merchant ship-radiated noise. *The Journal of the Acoustical Society of America*, 111(3), 1211–1231. <https://doi.org/10.1121/1.1427355>
47. Wang, L.S., Heaney, K., Pangerc, T., Theobald, P.D., Robinson, S.P., Ainslie, M. A, 2014. Review of underwater acoustic propagation models. NPL REPORT AC 12.

48. Wenz, G., 1962. Acoustic Ambient Noise in the Ocean : Spectra and Sources. J. Acoust. Soc. Am. 34, 21
49. William D. Halliday, Stephen J. Insley, R. Casey Hilliard, Tyler de Jong, Matthew K. Pine, Potential impacts of shipping noise on marine mammals in the western Canadian Arctic, In Marine Pollution Bulletin, Volume 123, Issues 1–2, 2017, Pages 73-82, ISSN 0025-326X, <https://doi.org/10.1016/j.marpolbul.2017.09.027>.
50. Zisis, D., Xidias, E.K., and Lekkas, D., Real-Time Vessel Behavior Prediction, Evolving Systems, vol. 7 pp. 29-40, 2016.



## 8 ANNEX I

### The FORTH Model

Skarsoulis, E.K., Piperakis, G.S., Orfanakis, E., Papadakis, P., and Taroudakis M., “Modelling of Underwater Noise Due to Ship Traffic in the Eastern Mediterranean Sea”, In proceedings of the 4th Underwater Acoustics Conference and Exhibition (UACE2017), pp. 889-896, (2017).

## Modelling of underwater noise due to ship traffic in the Eastern Mediterranean Sea

E. Skarsoulis<sup>a</sup>, G. Piperakis<sup>a</sup>, E. Orfanakis<sup>a</sup>, P. Papadakis<sup>a</sup>, M. Taroudakis<sup>b,a</sup>

<sup>a</sup> Institute of Applied and Computational Mathematics FORTH, Heraklion, Crete, Greece

<sup>b</sup> University of Crete, Department of Mathematics, Heraklion, Crete, Greece

**Abstract:** *A prediction model for shipping noise in the Eastern Mediterranean Sea is presented combining AIS data for ship locations/characteristics, environmental data and acoustic propagation codes. Taking into account typical acoustic emission characteristics of travelling ships, prevailing temperature and sound-speed distributions subject to seasonal variation, as well as the exact bathymetry in the area, range-dependent propagation calculations are carried out. Results for the geographical distribution of noise levels at various depths are produced and periodically updated on an hourly basis.*

**Keywords:** *Underwater noise, shipping noise, propagation modelling*

## 1. INTRODUCTION

Noise due to ship traffic is a substantial component of ambient noise in the sea, dominating in the low-frequency range, below 500 Hz. Travelling ships are sources of low-frequency acoustic waves which propagate efficiently through the water mass and thus affect underwater noise levels at large distances from the major shipping lanes.

In recent years the European Union introduced the Marine Strategy Framework Directive (MSFD) aiming at the establishment of good environmental status in the sea areas surrounding Europe [1]. The MSFD addresses, among others, underwater noise pollution and requires the monitoring of continuous low-frequency (63 and 125 Hz) noise through measurement by observation stations and/or with the use of models if appropriate.

The Eastern Mediterranean Sea is characterized by heavy ship traffic, with major shipping lanes connecting, among others, the Sicily Strait, the Adriatic Sea, the Black Sea and the Suez Canal. The measurement of ambient noise distribution over time and space in such a large sea area with complicated bathymetry and coastline poses serious challenges. Acoustic propagation modelling in combination with advancements in the availability of ship tracking data can be supportive in this respect.

The propagation of sound in water is influenced by changes in temperature and pressure (also by changes in salinity albeit to a much lesser extent). E.g. the warming of surface layers in summer causes strong sound-speed gradients leading to downward refraction and thus affect noise levels close to the surface [2]. The complicated bathymetry also plays a significant role in acoustic propagation giving rise to bottom losses and acoustic blockage effects.

In earlier times the lack of sufficient information about distant ship traffic was a hampering factor for operational modelling of shipping noise in open sea areas. In this connection early modelling approaches were mainly of statistical nature [3] or relied on certain navigation scenarios [4]. In recent times ship traffic data have become readily available through the Automatic Identification System (AIS) and the corresponding ship tracking services offering world-wide coverage [5].

The present work describes a prediction model for shipping noise in the Eastern Mediterranean Sea combining AIS data for ship locations/characteristics, environmental data and acoustic propagation codes. Typical acoustic emission characteristics of travelling ships are taken from the literature. A wave-theoretic range-dependent acoustic propagation model relying on adiabatic-mode theory is used. Concerning the environmental parameters, the seasonal temperature variation in the water column as well as the bathymetry and bottom composition are accounted for.

The geographical distribution of noise levels at various depths is estimated and periodically updated on an hourly basis. Some of the results can be found on the internet at the address <http://www.iacm.forth.gr/shipnoise>

## 2. AIS DATA

The primary purpose of the Automatic Identification System (AIS) is collision avoidance. All ships of 300 gross tonnage and above are equipped with VHF systems broadcasting their characteristics (ship name, type, location, navigation status, speed, etc.) and receiving the corresponding characteristics of nearby ships. In recent years, ship tracking services relying on land and satellite based AIS stations/receivers have been developed. In this way ship traffic data for any sea area are available in near real time. Information about ship type and navigation status contained in the AIS data can be used to infer on sound emission levels of each ship. By combining these data with the bathymetry characteristics and the prevailing propagation conditions in the area of interest and by applying acoustic propagation codes the distribution of noise in the area of interest can be estimated.

In the context of this work, an AIS receiver was installed at FORTH (Heraklion, Crete) and was integrated into the MarineTraffic network, a web-based ship tracking service ([www.marinetraffic.com](http://www.marinetraffic.com)). In response MarineTraffic kindly provides ship traffic data from terrestrial and satellite AIS receivers covering the Eastern Mediterranean Sea on a continuous basis. A typical picture of ship traffic in the area is shown in Fig. 1.

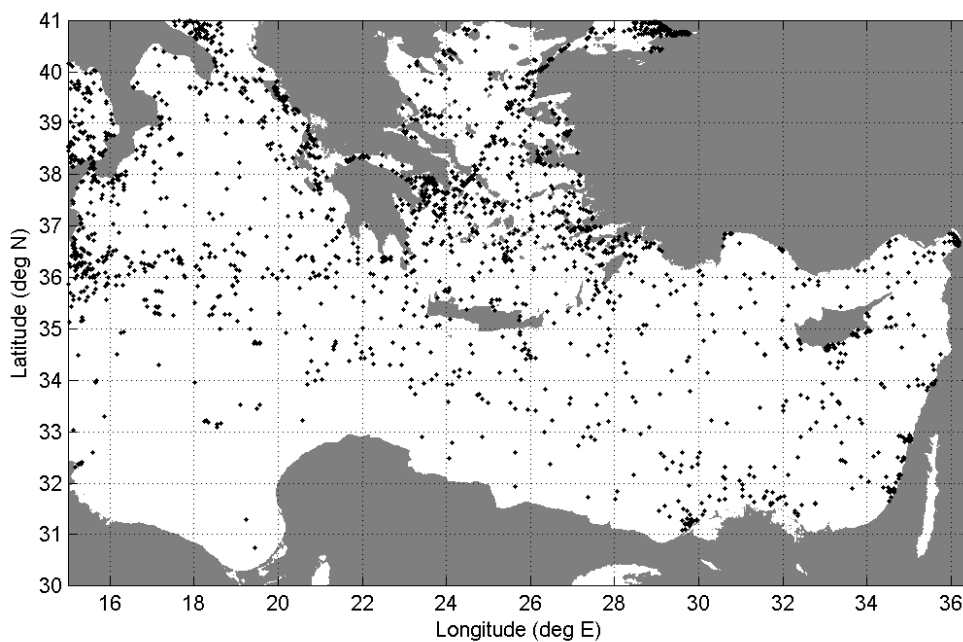


*Fig.1: Snapshot of ship traffic on 1 June 2017 in the Eastern Mediterranean Sea, based on AIS data.*

### 3. NOISE MODELING

#### 3.1 Source levels

Travelling ships are sources of underwater noise. The noise is generated by the propellers, the main engines and the auxiliary machinery, as well as by hull vibrations. The characteristics of the produced sound depend on ship type, design and construction, maintenance status, navigation conditions (speed, load, etc.). The emitted sound along a particular direction can be described by the source level spectral density as a function of frequency (acoustic signature) measured in dB re  $1 \mu\text{Pa}^2 / \text{Hz} @ 1\text{m}$ .

Data on acoustic signatures for different ship types can be found in the literature. Recent studies [6]-[9] are based on the combination and analysis of underwater acoustic measurements and simultaneous AIS data of large numbers of travelling ships, taking into account propagation characteristics of the measurement sites. Despite the detailed analyses the reported spectral levels are characterized by large variability, reaching 25 dB in some cases. These differences may be due to the different measurement setups and travelling vessels involved at the different locations.

The spectral source level values given by McKenna et al. [6] and Basset et al. [7] lying close to the middle of the variability intervals are used in the following as the basis for noise predictions at the frequency of 100 Hz. According to those studies, average spectral source levels are about 155 dB re  $1 \mu\text{Pa}^2/\text{Hz} @ 1\text{m}$  for tankers and cargo ships, 150 dB re  $\mu\text{Pa}^2/\text{Hz} @ 1\text{m}$  for passenger ships, 145 dB re  $1 \mu\text{Pa}^2/\text{Hz} @ 1\text{m}$  for fishing vessels, 140 dB re  $1 \mu\text{Pa}^2/\text{Hz} @ 1\text{m}$  for auxiliary vessels.

Ideally, each individual ship should have its own set of acoustic signatures corresponding to different navigation / load conditions and different azimuthal directions, which should also be updated from time to time. Such detailed data are collected for some types of naval vessels – and usually remain classified – but are not available for commercial vessels. In any case the focus of the present work is not on the acoustic signatures but rather the pilot application of AIS data for real-time estimation of ambient noise levels over a broad area. Better and more representative acoustic signatures for the involved vessels will lead to more accurate noise estimation results. In the lack of such data the typical sound emission levels mentioned above will be used.

#### 3.2 Acoustic propagation

For long-range propagation calculations each ship is considered as an omnidirectional source (point source) at a depth of 9 m, an average depth [7], [9] taking into account that ship draught values may vary from a few meters up to about 20 m for large vessels under full load.

The bathymetry of the Eastern Mediterranean Sea is taken from the ETOPO1 database; this is a 1 arc-minute global relief model of Earth's surface that integrates land topography and ocean bathymetry. For the acoustic calculations a 2/60 deg grid is adopted (resolution 3.6 km). Ship positions in the horizontal are rounded to the nearest grid point and their acoustic intensities are accumulated assuming incoherence.

A simplified model is used for the temperature distribution assuming seasonal dependence and dependence with depth. Further the bottom is considered to be homogenous and acoustic with sound speed 1800 m/s, density 2 gr/cm<sup>3</sup> and attenuation 1 dB/λ. Thus, range dependence is only due to bathymetry. For the calculation of the acoustic field the KRAKEN normal-mode code [10] is used and the adiabatic approach [11], [12] is applied. The fact that different locations differ only in the water depth allows for categorization of different areas according to the water depth and the use of precalculated eigenvalues and eigenfunctions to accelerate calculations.

The seasonal variation of the temperature (and sound speed) profile is taken into account through a parametric model combining a linear velocity profile, 1510 m/s at the surface and 1570 m/s at 4000 m depth (typical winter profile in the Mediterranean), and a linear heating profile for the upper 150 m layer, starting from zero at 150 m depth and reaching its maximum at the surface. The velocity variation on the surface is taken between 1510 m/s (winter - zero heating) and 1545 m/s (summer - maximum heating).

Thus, on each day of the year a typical temperature (and sound-speed) profile is calculated which determines the acoustic environment. For this environment the eigenvalues and propagating modes are calculated and stored for different water depths to cover all areas of interest, from the shallowest to the deepest. Then for every hour of the day, corresponding to a different source distribution, the acoustic field at any location (receiver location) in the basin is calculated by combining eigenvalues and eigenfunctions at each source and each receiver location, as well as at the locations along the path connecting source and receiver, retaining the minimum number of propagating modes along the path (mode stripping), and incoherently adding the acoustic intensities contributed by the various sources. The number of sources (ship groups) in the Eastern Mediterranean Sea typically ranges between 1500 and 3000, whereas the number of grid points (3.6 m resolution), where the acoustic field is calculated, is about 120000, resulting in a very large number of source-receiver combinations. In this connection the acoustic field calculations are carried out on a cluster using a parallel computation scheme.

#### 4. NUMERICAL RESULTS

Some results are presented in the following for the predicted noise levels due to shipping in the Eastern Mediterranean Sea. The ship distribution of Fig. 1, counting a total of 2130 ship groups, is used as the basis for the calculations. Fig. 2 shows the 5% and 95% percentile values, i.e. the noise levels exceeded 95% and 5% of the time respectively, at a



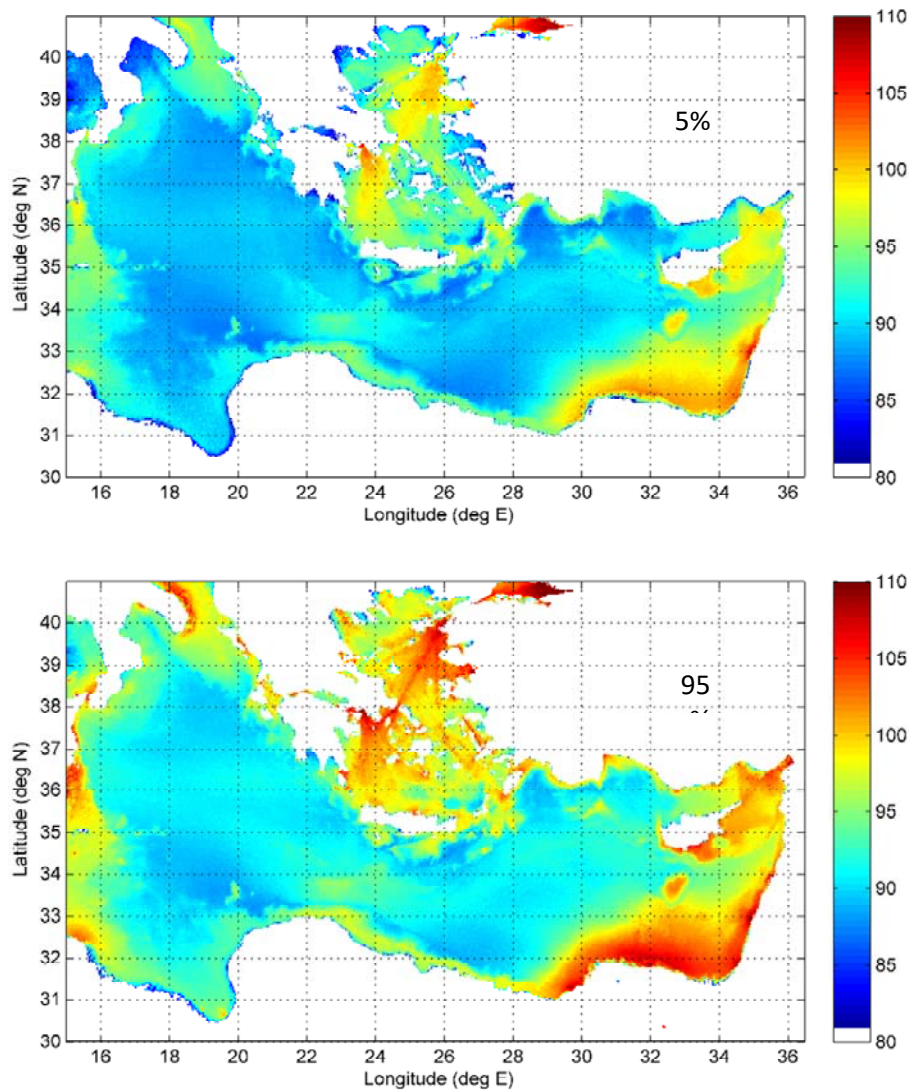


*Fig.2: Predicted spectral noise level (dB re  $1\mu\text{Pa}^2/\text{Hz}$ ) distribution on 1 June 2017 in the Eastern Mediterranean at the depth of 50 m and frequency of 100 Hz – 5% (top) and 95% (bottom) percentile values over 24 h.*

depth of 50 m and frequency of 100 Hz. It is interesting to see that the noise levels are high in shallow water areas, close to major ports and shipping lanes, e.g. in the south-eastern part of the basin near the port of Alexandria and the entry of the Suez canal or in the Aegean Sea, whereas they are lower in the deep-water areas of the Eastern Mediterranean Sea, e.g. in the deep Ionian basin. A physical explanation of this behaviour can be given in terms of the lower amplitudes of the propagating modes in deep water, as contrasted to the higher amplitudes in shallow water. The major shipping routes can be identified in the 95% percentile results.

In order to see the effect of the propagation characteristics on the noise level distribution, Fig. 3 shows the predicted spectral noise levels for the ship distribution of Fig. 1 using two extreme sound-speed profiles, the winter linear profile and the summer profile with maximum heating at the surface. The first sound-speed profile is upward



refracting, whereas the second one has a minimum at 150 m depth and a strong temperature (sound-speed) gradient causing downward refraction at shallower depths. It is seen in Fig. 3 that the noise levels at 50 m depth in summer are much lower than in winter,

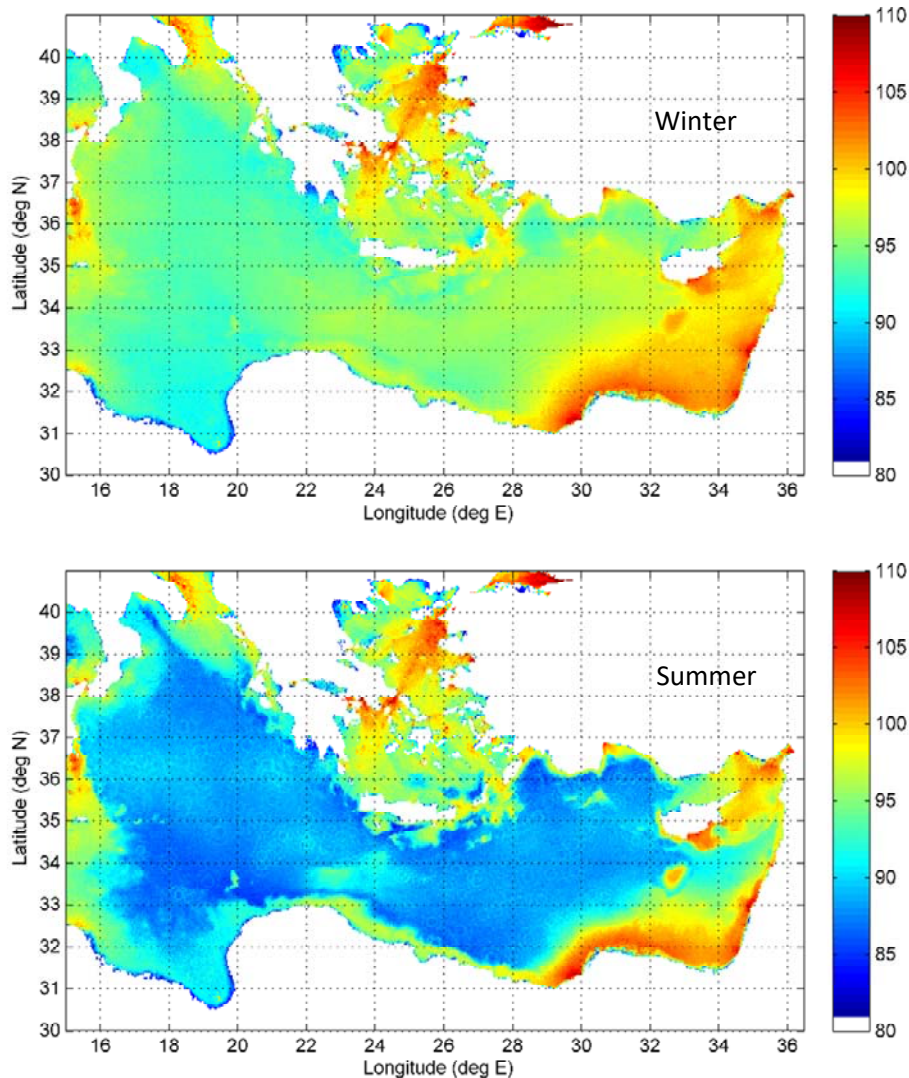


*Fig.3: Predicted spectral noise level (dB re 1µPa<sup>2</sup>/Hz) distribution at the depth of 50 m and frequency of 100 Hz, corresponding to the ship traffic of Fig. 1 assuming winter (top) and summer (bottom) propagation conditions.*

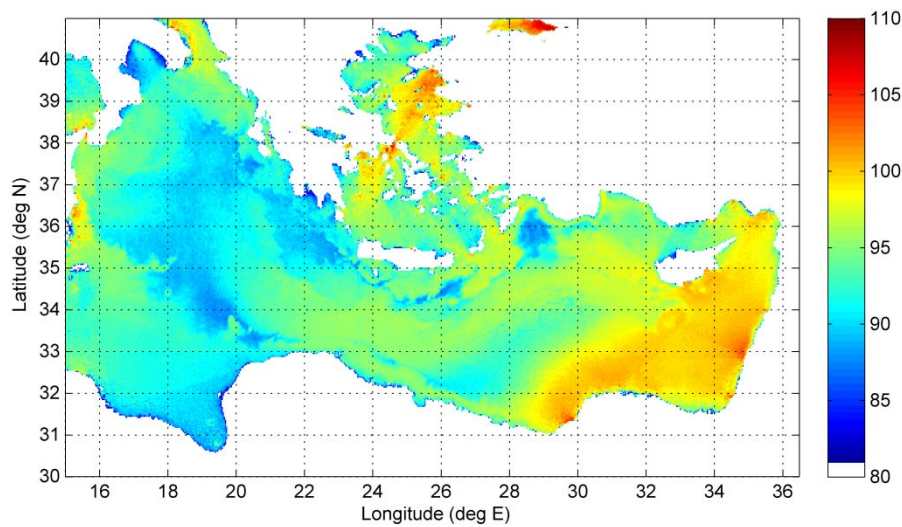


*Fig.4: Predicted spectral noise level (dB re  $1\mu\text{Pa}^2/\text{Hz}$ ) distribution at the depth of 100 m and frequency of 100 Hz, corresponding to the ship traffic of Fig. 1 assuming summer propagation conditions.*

especially in the deep-water parts of the basin. This is the effect of the strong downward refraction taking place in summer in the upper layers, where the sound sources are located. It is remarkable that this refraction effect is felt so clearly by the low frequency of 100 Hz (wavelength of 15 m). Based on the above argumentation the acoustic energy in summer should be found in deeper layers. Fig. 4 shows the predicted spectral noise level at a depth of 100 m. It is clear from this figure that the acoustic energy is directed to the deep. Results like these are produced on a systematic and continuous basis and are updated hourly and can be accessed at [www.iacm.forth.gr/shipnoise](http://www.iacm.forth.gr/shipnoise).

## 5. CONCLUSION / SUMMARY

The measurement of ambient noise distribution over large sea areas with complicated bathymetry and coastline such as the Eastern Mediterranean Sea and its variability in time and space poses serious challenges. Acoustic modelling can be supportive in this respect. The combination of propagation models with environmental and AIS data enables the prediction of shipping noise distribution in near-real time and allows for the study of the influence of various factors, e.g. environmental variability or acoustic emission characteristics. A combination of prediction models with actual noise measurements at selected locations (ground truth) is the most appropriate approach for monitoring noise levels over large sea areas with the complex characteristics of the Mediterranean Sea.

In this work a normal-mode approach (adiabatic approximation) is combined with AIS data and typical emission characteristics using a simple environmental model accounting for the bathymetry of the Eastern Mediterranean Sea to produce predictions of the shipping noise distribution at various depths in near-real time. Applications of the

results include the environmental characterization of particular marine areas, the analysis of the behavior of submarine sonar systems, etc.

A significant source of uncertainty for the obtained noise level results has to do with the acoustic emission characteristics of the contributing ships. Each particular vessel has a different emission level and directivity pattern depending on its design, maintenance status, load, navigation conditions. Acoustic models such as the one presented here can account for all these characteristics. Nevertheless, the presently available data on acoustic emissions refer to typical levels depending on ship type, subject to a large amount of uncertainty. The significance of the accurate knowledge of the emission characteristics and its impact on noise estimation accuracy can be assessed with modelling.

## 6. ACKNOWLEDGEMENTS

This work was carried out in the framework of the Hellenic Republic - Siemens agreement partially funded by the Programmatic Agreement between Research Centers and the General Secretariat for Research and Technology (GSRT) 2015-2017 and was further supported by the QUIETMED research project.

## REFERENCES

- [1] AJ Van der Graaf, MA Ainslie, M André, K Brensing, J Dalen, RPA Dekeling, S Robinson, ML Tasker, F Thomsen, and S Werner, *European Marine Strategy Framework Directive - Good Environmental Status (MSFD GES): Report of the Technical Subgroup on Underwater noise and other forms of energy*, 2012.
- [2] M. Taroudakis, A Study of the Influence of the Environmental Parameters on the Traffic Noise in the Sea, *Colloque De Physique*, No 2, Supplement, Tome 51, Pp C2.1001-C2.1004, 1990
- [3] P.N. Mikhalevsky, and I. Dyer, Approximations to Distant Shipping Noise Statistics. *J Acoust Soc Am.*, vol. 63, pp. 732-738, 1978.
- [4] M.I. Taroudakis, and N.X. Nikolaidis, A Simplified Model for the Estimation of the Traffic Noise in Shallow Water, *Technika Chronika – Scientific Edition B*, vol. 9, pp. 47-72, 1989.
- [5] D. Zissis, E.K. Xidias, and D. Lekkas, Real-Time Vessel Behavior Prediction, *Evolving Systems*, vol. 7 pp. 29-40, 2016.
- [6] M. F. McKenna, D. Ross, S. M. Wiggins, and J. A. Hildebrand, Underwater radiated noise from modern commercial ships, *J. Acoust. Soc. Am.*, vol. 131, pp. 92–103, 2012.
- [7] C. Bassett, B. Polagye, M. Holt, and J. Thomson, A Vessel Noise Budget for Admiralty Inlet, Puget Sound, Washington (USA), *J. Acoust. Soc. Am.*, vol. 132, pp. 3706–3719, 2012.
- [8] S. Veirs, V. Veirs, and J. D. Wood, Ship Noise Extends to Frequencies Used for Echolocation by Endangered Killer Whales, *PeerJ*, vol. 4, e1657, 2016.

- [9] Y. Simard, N. Roy, C. Gervaise, and S. Giard, Analysis and Modeling of 255 Ship Source Levels from an Acoustic Observatory Along St. Lawrence Seaway, *J. Acoust. Soc. Am.*, vol. 140, pp. 2002–2018, 2016.
- [10] M. Porter, and E.L. Reiss. A Numerical Method for Ocean Acoustic Normal Modes, *J. Acoust. Soc. Am.*, vol. 76, pp. 244-252, 1984.
- [11] F. B. Jensen, W. A. Kuperman, M. B. Porter, and H. Schmidt, *Computational Ocean Acoustics*, American Institute of Physics, Melville, NY, 1994.
- [12] M. Porter, and L. Henderson, Global Ocean Soundscapes, in *Proceedings of Meetings on Acoustics*, vol. 19, 010050, pp. 1-6, 2013.